Title

Qurliqnoria (Mammalia: Bovidae) fossils from Qaidam Basin, Tibetan Plateau and deep-time endemism of the Tibetan antelope lineage

Permalink

https://escholarship.org/uc/item/4vc6f7hf

Journal

Zoological Journal of the Linnean Society, 196(3)

ISSN

0024-4082

Authors

Tseng, Z Jack
Wang, Xiaoming
Li, Qiang
et al.

Publication Date

2022-11-02

DOI

10.1093/zoolinnean/zlab117

Peer reviewed

Qurliqnoria (Mammalia: Bovidae) fossils from Qaidam Basin, Tibetan Plateau and deep-time endemism of the Tibetan antelope lineage

Z. JACK TSENG[1,2,*], XIAOMING WANG[2,3], QIANG LI[3,4,5] and GUANGPU XIE[6]

[1]*Department of Integrative Biology and Museum of Paleontology, University of California, Berkeley, CA 94720, California, USA*
[2]*Department of Vertebrate Paleontology, Natural History Museum of Los Angeles County, 900 Exposition Boulevard, Los Angeles, CA 90007, California, USA*
[3]*Key Laboratory of Vertebrate Evolution and Human Origins, Institute of Vertebrate Paleontology and Paleoanthropology, Chinese Academy of Sciences, Beijng 100044, China*
[4]*CAS Center for Excellence in Life and Paleoenvironment, Beijing 100044, China*
[5]*University of Chinese Academy of Sciences, Beijing 100049, China*
[6]*Natural Science Department, Gansu Provincial Museum, No. 3 Xijingxi Road, Lanzhou 730050, Gansu, China*

The Tibetan antelope (*Pantholops hodgsonii*) is an endemic bovid of the Tibetan Plateau, which was, until recently, considered an endangered species. Researchers have long speculated on the evolutionary origin of *Pantholops*, suggesting a connection to the rare fossil bovid *Qurliqnoria*. However, the lack of adequate fossil samples has prevented the testing of this deep-time endemism hypothesis for eight decades. Here, we report new fossils of *Qurliqnoria cheni* from the northern Tibetan Plateau, substantially increasing the amount of morphological data that can be brought to bear on the question of Tibetan antelope evolution. Phylogenetic analysis supports a *Pantholops–Qurliqnoria* clade and suggests that this lineage has been endemic to the Plateau for 11 Myr. Recent morphological and molecular studies that support the outgroup position of *Pantholops* relative to caprins (goats and relatives) and the fossil record of stem bovids from Europe together suggest that the *Qurliqnoria–Pantholops* lineage is likely to have dispersed to the Tibetan Plateau 15–11 Mya. Furthermore, the harsh environmental conditions to which *Pantholops* has adapted are likely to extend back to the time of its evolutionary origin. These findings provide an important new context for conservation management and research into the near-threatened Tibetan antelope, as the longest-living endemic member of the Tibetan Plateau fauna.

ADDITIONAL KEYWORDS: Caprini – chiru – climate change – conservation – endangered species – endemic species – fossil record – Miocene.

INTRODUCTION

The Tibetan antelope or chiru, *Pantholops hodgsonii* (Abel, 1826), is one of several endangered mammal species found on the Tibetan Plateau of Central Asia (IUCN Red List of Threatened Species; https://www.iucnredlist.org). Along with the snow leopard, *Panthera uncia* (Schreber, 1775), and Himalayan blue sheep, *Pseudois* Hodgson, 1846 spp., the chiru is found year-round on the Plateau and can handle its harsh winters (Leslie & Schaller, 2008). Found at elevations of 3250–5550 m a.s.l., the chiru is adapted to hypoxic and hypothermic conditions, as evidenced by gene expressions associated with energy metabolism and oxygen transmission (Ge *et al.*, 2013; Signore & Storz, 2020) and by their dense wool with thin walls and internal space exhibiting a unique benzene-ring-like shape (Leslie & Schaller, 2008).

Early explorers remarked about the chiru being the most abundant large mammal on the Tibetan

*Corresponding author. E-mail: zjt@berkeley.edu

Plateau (Rawling, 1905; Schaller, 1998). However, intensive poaching during the 20th century, mostly to profit from the much sought-after fine wool of the chiru, used in luxury Kashmir shawls ('shahtoosh'), had reduced their populations by ≥ 90% (Leclerc *et al.*, 2015). Although there has been evidence of population recovery resulting from conservation efforts in the past two decades, moving the chiru to Near Threatened status from Endangered (IUCN SSC Antelope Specialist Group, 2016), the compounding effects of ongoing climate change are bringing this species back to the brink of endangerment (Pei *et al.*, 2019).

The rapidly developing field of conservation palaeobiology, the study of biodiversity conservation using palaeontological data and approaches, is being recognized as an important component of current conservation research (Dietl, 2016; Barnosky *et al.*, 2017). The evolutionary and zoogeographical origins of threatened species inform their management and conservation by contextualizing the deep-time history of their interactions with long-term environmental and ecological shifts. However, unlike the recently clarified evolutionary history of snow leopards based on fossil discoveries in the northern Himalayan foothills (Tseng *et al.*, 2014), the evolutionary origin of the chiru has proved to be more elusive.

In a commentary penned more than five decades ago, Alan Gentry (1968) speculated on the deep-time connection of *Pantholops* Hodgson, 1834 to the fossil bovid *Qurliqnoria* Bohlin, 1937. In the intervening 80+ years since the original two specimens of *Qurliqnoria cheni* Bohlin, 1937 were discovered and subsequently published by Swedish explorer and palaeontologist Birger Bohlin (Bohlin, 1937), no substantial new fossil samples of this extinct bovid have been reported from the Tibetan Plateau until now. In this report, we describe and discuss two dozen new *Qurliqnoria* fossils found in the Qaidam Basin, northern Tibetan Plateau.

For nearly 70 years after Bohlin's publication, the exact locality of *Qurliqnoria* fossils remained unclear, despite repeated attempts by some of us to relocate it, and as a result, their stratigraphic position and geological age were a source of much confusion and speculation. In 2007, we finally made a positive identification of Bohlin's original localities near the present-day Quanshuiliang railroad station (Wang *et al.*, 2007) in the Qaidam Basin. Our own subsequent fieldwork in the Quanshuiliang area resulted in a large collection of additional fossil material, the richest of which are two dozen horncores and crania belonging to *Q. cheni*. These fossils substantially improve our knowledge of this extinct bovid and are crucially informative for clarifying the evolutionary origin of the chiru. The new data support the interpretation of an endemic lineage surviving in the high Tibetan Plateau for ≥ 10 Myr.

GEOLOGICAL AND PALAEONTOLOGICAL CONTEXT

The Qaidam Basin is the largest Cenozoic basin on the Tibetan Plateau (Fig. 1). The Basin is ~550 km (east–west) by ~250 km (north–south) in maximum dimensions and has accumulated, at its depositional centre, > 15 000 m of fluviolacustrine sediments encompassing the Palaeocene–Early Eocene to the present (Wang *et al.*, 2007; Yin *et al.*, 2007, 2008a, b). The earliest documented Qaidam fossils were those studied by Birger Bohlin, chief vertebrate palaeontologist of the Sino-Swedish Expeditions (Bohlin, 1945). Large mammal fossils from the Tuosu Nor and surrounding areas in the eastern Qaidam Basin were described, representing the first major fossil vertebrate collection from the Tibetan Plateau, which are still being used as the main framework of Late Cenozoic biostratigraphy and geochronology in the region (Wang *et al.*, 2011). Of these, four bovid species, *Olonbulukia tsaidamensis* Bohlin, 1937, *Q. cheni*, *Tossunnoria pseudibex* Bohlin, 1937 and *Tsaidamotherium hedini* Bohlin, 1935, feature peculiar morphologies that were thought to be indicative of taxa endemic to the Tibetan Plateau and therefore possessing special zoogeographical significance (Bohlin, 1935a, 1937).

Bohlin took detailed field notes during his 1931 and 1932 expeditions to the Qaidam Basin. His notebooks are deposited in the Swedish National Archives (Stockholm) and have been translated fully by Wang *et al.* (2011). In addition, sketch maps drawn by Bohlin were also interpreted in a modern stratigraphic context by Wang *et al.* (2011). As a result, nearly all of the fossils published in Bohlin's (1937) monograph can be located on his maps and be correlated roughly to a 4500 m palaeomagnetic section in nearby Huaitoutala (Fang *et al.*, 2007; Wang *et al.*, 2007).

MATERIAL AND METHODS

The phylogeny of Bovidae is difficult to resolve using morphology alone, and conflict between morphological and molecular data persists across tribes (Bibi, 2013). Therefore, our approach is to sample a range of constrained phylogenetic scenarios and evaluate the support for a particular placement of *Qurliqnoria* using comparisons of a sample of parsimony trees, analogous to a model-based approach to phylogenetic analysis (Mathews *et al.*, 2010; Lee, 2013; Field & Hsiang, 2018). Cladistic analyses were conducted in TNT v.1.5 (Goloboff & Catalano, 2016) using the 'New Technology' search strategy. The character matrices were built in MESQUITE v.2.71 (Maddison & Maddison, 2009). The core characters
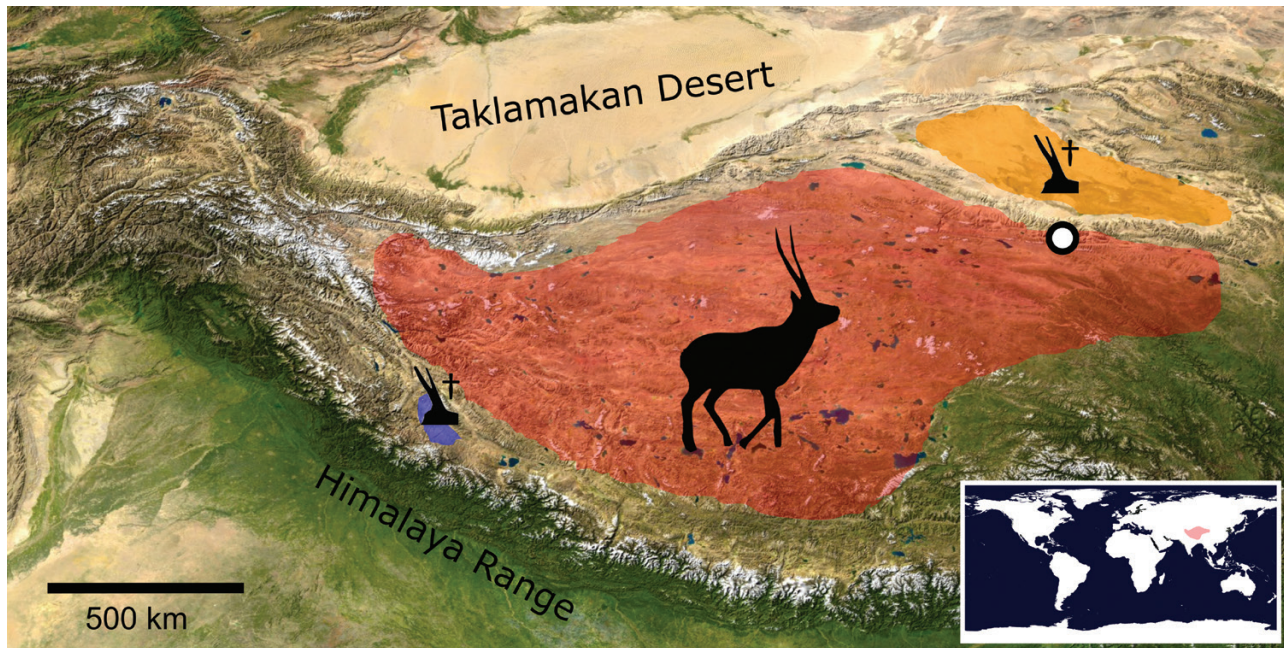
Figure 1. Satellite map of the Tibetan Plateau region. The current geographical distribution of the Tibetan antelope is shaded in red (data from IUCN SSC Antelope Specialist Group, 2016). Fossil occurrences discussed in this paper are from Qaidam Basin (orange area), Zanda Basin (blue area) and Kunlun Pass Basin (circle). The satellite image and world map are modified from NASA; silhouettes are modified from PhyloPic.org.

and taxa used in analysis follow Gentry (1992). A total of 57 parsimony-based analyses that incorporate different degrees of backbone topological constraints from the recently established molecular phylogeny of Bovidae (Bibi, 2013) were conducted to test the support for a *Qurliqnoria–Pantholops* clade (see Character Matrix section below). Analyses for cranial and horncore specimens vs. referred dental material of *Qurliqnoria* were conducted both separately and as one taxonomic unit. Horncore and cranial measurements were taken with Mitutoyo vernier callipers to the nearest 0.2 mm. Dental measurements were taken to the nearest 0.1 mm.

Institutional abbreviations for specimen repositories are as follows: IVPP, Institute of Paleontology and Paleoanthropology, Chinese Academy of Sciences, Beijing, China; NHMUK, Natural History Museum, London, UK; and NMNH, National Museum of Natural History (Smithsonian Institution), Washington, DC, USA. Taxonomic names for bovid clades are based on those used by Bibi (2013).

CHARACTER MATRIX

The character matrix from Gentry (1992) was modified and used as the core character matrix in a series of sensitivity analyses incorporating different topological constraints. In all analyses, we treated Bovinae taxa as the outgroup to the rest of Bovidae (Antilopinae); *Tetracerus* Leach, 1825 was used as

the outgroup taxon. Given that analyses in TNT allow only a single outgroup taxon, three Bovinae taxa from Gentry's matrix were removed from the analyses (*Bison* Hamilton Smith, 1827, *Boselaphus* Blainville, 1816 and *Tragelaphus* Blainville, 1816). Analysis set A (defined in next paragraph) was run iteratively with each one of the excluded Bovinae taxa as the outgroup instead of *Tetracerus*; the resulting topologies and relative tree lengths were consistent with results obtained from using *Tetracerus* as the outgroup. Therefore, only analyses using *Tetracerus* as the outgroup are reported. Furthermore, we removed *Ammodorcas* Thomas, 1891 from the analyses, because there is no reliable molecular topology incorporating this taxon available. Our final modified core matrix included 23 taxa and 112 unordered characters.

Four major sets of phylogenetic analysis using parsimony were conducted by adding *Qurliqnoria* to the core matrix and: (1) using the full 112-character matrix with 23 core taxa plus *Qurliqnoria*, with only cranial and horncore characters being coded for *Qurliqnoria* (analysis set A); (2) adding 12 additional fossil bovids partly coded for the cranial and horncore characters by Gentry (1992), resulting in a matrix of 36 taxa (analysis set B); (3) using the full dataset of 112 characters with 23 core taxa plus *Qurliqnoria* and coding for dental characters only using the referred fossil specimens described in the present study; and (4) combining analysis sets A and C, coding *Qurliqnoria* for both

cranial and dental characters, with the speculation that the specimens described herein belong to a single taxon (analysis set D). Given the lack of a direct association between the horncore and dental fossil material described in the present study, the results from analysis set D should be interpreted with caution.

For each analysis set, 14 different scenarios were tested (Table 1). These analyses tested the effects of a strict backbone scaffold vs. a series of clade-specific constraints for the position of *Qurliqnoria*. Given that each of the analysis sets included different combinations of character matrix and taxonomic sample size, the parsimony scores were compared between different scenarios within each analysis set, but not across them. The trees with the lowest parsimony scores, suggesting the least number of evolutionary changes required given a tree topology, were considered the best-supported tree topologies under a parsimony criterion and used for further discussion and interpretation. To aid the direct comparison of tree scores across the different analysis sets, parsimony scores between scenarios where *Qurliqnoria* and *Pantholops* belonged in the same clade vs. different clades were evaluated statistically using Kruskal–Wallis tests (= non-parametric ANOVA), with scores scaled to a mean of zero and standard deviation of one within each analysis set.

All character matrices generated in this study are deposited in the Morphobank database (https://morphobank.org/index.php/Projects/ProjectOverview/project_id/4010).

SYSTEMATIC PALAEONTOLOGY

Class Mammalia Linnaeus, 1758
Order Artiodactyla Cope, 1889
Family Bovidae Gray, 1821
Subfamily Antilopinae Gray, 1821
Qurliqnoria cheni Bohlin, 1937
(Figs 2–4; Tables 2 and 3)

Qurliqnoria cheni Bohlin, 1937: 34–36, plate III, figs 6, 7; Qiu *et al.*, 1987: 51–52, fig. 4.
Qurliqnoria sp. Bohlin, 1937: 36–37, plate IV, figs 1, 2.

Holotype: IVPP *RV37100*, broken cranium with partial horncores. From the eastern end of the 'General Strips' at point 183 in the eastern Qaidam Basin (Bohlin, 1937).

Referred material: IVPP V16949, partial cranium missing the portion rostral to the frontal bones, with the base of both horncores preserved; IVPP V16952, partial cranium missing the palate rostral to the orbits, with left horncore preserved; IVPP V27838, V16947–V16948, V16950, V16955 and V16963, partial left horncores; IVPP V16941, V16943–V16944, V16951, V16954, V16957–V16958, V16962 and V16964, partial right horncores; IVPP V16942 and V16959–V16960, frontal fragments with partial left and right horncores.

Emended diagnosis: Medium-sized bovid about the size of extant *Pantholops*, with shorter horncores than *Pantholops* and more distinct mediolateral compression; horncore pedicle short, base of horncores close together rostrally; horncores form an angle of 90° with the cranial roof (measured between the posterior horncore and the dorsal edge of the parietal bone in lateral view); interfrontal suture complicated but not raised as a ridge between the pedicles; dorsal orbital rim laterally expanded; inflated bulla, triangular to trapezoidal basioccipital bone with central constriction; mastoid does not contact parietal; strong longitudinal grooves along the length of the horncore; similar to *Pantholops* in strong lateral compression at the distal region of the horncores, the presence of anterior keels, stronger longitudinal grooves on the posterior part of the horncores, upright insertion of the horncores on the skull and little backward curvature distally, short pedicel, closely set supraorbital foramina which are simple pits, potentially wide orbital rims and frontal sinus not expanded. Similar to *Dorcadoryx* Teilhard de Chardin & Trassaert, 1938, *Huabeitragus* Chen & Zhang, 2007 and *Macrotragus* Chen & Zhang, 2007 in having a triangular occipital, transversely compressed horncores and presence of an anterior keel on horncores.

Qurliqnoria cheni differs from other Qaidam medium to large bovids (*Tossunnoria* and *Olonbulukia*) in the following characters: horncores moderately divergent in rostral view, not greatly divergent as in *Tossunnoria* or parallel as in *Olonbulukia*; presence of homonymous torsion on horncore, not straight as in *Olonbulukia*; deep longitudinal grooves present on horncores, not smooth as in *Olonbulukia*; parietal and interparietal parts of the cranial roof convex dorsally, and the roof forms an obtuse angle with the occipital, not flattened cranial roof and sharper angle (~90–100°) as in *Olonbulukia*. Differs from Late Miocene bovids *Protoryx* Forsyth Major, 1891 and *Pachytragus* Schlosser, 1904 in smaller size, less posterior curvature of distal horncores and lack of raised interfrontal ridges; differs from the Middle Miocene *Tethytragus* Azanza & Morales, 1994 in longer horncores, larger degree of mediolateral horncore compression and larger size; differs from two tentative fossil *Pantholops* horncore specimens from the Zanda Basin (ZD0745 and ZD0904) and one skeletal specimen of extant *Pantholops* observed in the Kunlun Pass Basin in having more deeply longitudinally grooved horncore surface rather than a shallow or smooth surface.

Table 1. Sensitivity analyses of phylogenetic scenarios and resulting parsimony scores. Scores are ranked within each analysis set (A–D) from lowest (most parsimonious) to highest (least parsimonious).

Scenario	Phylogenetic analysis definition	Score	*Qurliqnoria* position
	23 extant spp. + *Qurliqnoria* (skull morphology)		
A05	Mitochondrial DNA backbone: monophyly of tribes only, *Qurliqnoria* within Caprini + *Pantholops*	490	Sister to *Pantholops*
A08	Mitochondrial DNA backbone: monophyly of tribes only; *Qurliqnoria* in Hippotragini–Alcelaphini–Caprini–Reduncini stem	493	(See definition)
A03	Mitochondrial DNA backbone + *Qurliqnoria* forced as *Pantholops–Qurliqnoria* stem to monophyletic Caprini clade	494	Sister to *Pantholops*
A04	Mitochondrial DNA backbone + *Qurliqnoria* forced within monophyletic Caprini + *Pantholops* clade	494	Sister to *Pantholops*
A06	Mitochondrial DNA backbone: monophyly of tribes only; *Qurliqnoria* released from constraint	496	Most basal ingroup
A07	Mitochondrial DNA backbone: monophyly of tribes only, with *Qurliqnoria* in ingroup stem	496	Most basal ingroup
A02	Mitochondrial DNA backbone + relaxed Caprini monophyly	500	Most basal ingroup
A12	Mitochondrial DNA backbone + *Qurliqnoria* constrained to (*Ourebia, Saiga, Antilope, Gazella*)	515	(See definition)
A09	Mitochondrial DNA backbone + *Qurliqnoria* constrained to (*Aepyceros, Neotragus*)	516	(See definition)
A13	Mitochondrial DNA backbone + *Qurliqnoria* constrained to (*Kobus, Pelea*)	516	(See definition)
A14	Mitochondrial DNA backbone + *Qurliqnoria* constrained to (*Hippotragus, Damaliscus*)	516	(See definition)
A01	Mitochondrial DNA backbone without boselaphine, tragelaphine or bovine monophyly	519	Most basal ingroup
A10	Mitochondrial DNA backbone + *Qurliqnoria* constrained with (*Silvicapra, Oreotragus*)	520	(See definition)
A11	Mitochondrial DNA backbone + *Qurliqnoria* constrained with (*Raphicerus* (*Dorcatragus, Madoqua*))	521	(See definition)
	23 extant spp. + 12 additional fossil taxa + *Qurliqnoria* (skull morphology)		
B05	13 fossils + extant, backbone as in A5	519	Sister to *Pantholops*
B08	13 fossils + extant, backbone as in A8	522	(See A8 definition)
B03	13 fossils + extant, backbone as in A3	523	Sister to *Pantholops*
B04	13 fossils + extant, backbone as in A4	523	Sister to *Pantholops*
B06	13 fossils + extant, backbone as in A6	523	Sister to *Miotragocerus*
B07	13 fossils + extant, backbone as in A7	525	Most basal ingroup
B02	13 fossils + extant, backbone as in A2	527	Sister to *Miotragocerus*
B12	13 fossils + extant, backbone as in A12	544	(See A12 definition)
B09	13 fossils + extant, backbone as in A9	545	(See A9 definition)
B13	13 fossils + extant, backbone as in A13	545	(See A13 definition)
B14	13 fossils + extant, backbone as in A14	545	(See A14 definition)
B01	13 fossils + extant, backbone as in A1	546	Sister to *Miotragocerus*
B10	13 fossils + extant, backbone as in A10	549	(See A10 definition)
B11	13 fossils + extant, backbone with as in A11	550	(See A11 definition)
	23 extant spp. + *Qurliqnoria* (dental morphology)		
C05	Dental morphology + backbone as in A5	489	Polytomy with *Pantholops* + Caprini
C08	Dental morphology + backbone as in A8	489	(See A8 definition)
C06	Dental morphology + backbone as in A6	492	Ingroup stem
C07	Dental morphology + backbone as in A7	492	Ingroup stem

Table 1. Continued

Scenario	Phylogenetic analysis definition	Score	*Qurliqnoria* position
C03	Dental morphology + backbone as in A3	493	Sister to *Pantholops*
C04	Dental morphology + backbone as in A4	493	Polytomy with *Pantholops* + Caprini
C02	Dental morphology + backbone as in A2	496	Most basal ingroup
C12	Dental morphology + backbone as in A12	509	(See A12 definition)
C13	Dental morphology + backbone as in A13	509	(See A13 definition)
C14	Dental morphology + backbone as in A14	511	(See A14 definition)
C09	Dental morphology + backbone as in A9	512	(See A9 definition)
C01	Dental morphology + backbone as in A1	515	Most basal ingroup
C10	Dental morphology + backbone as in A10	515	(See A10 definition)
C11	Dental morphology + backbone as in A11	517	(See A11 definition)
	23 extant spp. + *Qurliqnoria* (dental + skull morphology)		
D05	Dental + skull morphology + backbone as in A5	494	Sister to *Pantholops*
D08	Dental + skull morphology + backbone as in A8	497	(See A8 definition)
D03	Dental + skull morphology + backbone as in A3	498	Sister to *Pantholops*
D04	Dental + skull morphology + backbone as in A4	498	Sister to *Pantholops*
D06	Dental + skull morphology + backbone as in A6	503	Ingroup stem
D07	Dental + skull morphology + backbone as in A7	503	Ingroup stem
D02	Dental + skull morphology + backbone as in A2	507	Most basal ingroup
D13	Dental + skull morphology + backbone as in A13	517	(See A13 definition)
D12	Dental + skull morphology + backbone as in A12	519	(See A12 definition)
D09	Dental + skull morphology + backbone as in A9	520	(See A9 definition)
D14	Dental + skull morphology + backbone as in A14	521	(See A14 definition)
D01	Dental + skull morphology + backbone as in A1	526	Most basal ingroup
D10	Dental + skull morphology + backbone as in A10	527	(See A10 definition)
D11	Dental + skull morphology + backbone as in A11	530	(See A11 definition)

Localities: The referred specimens were found throughout the area of 'General Strips' of Birger Bohlin (Bohlin, 1937, 1945; Wang *et al.*, 2011) or the area of the 'Quanshuiliang Fauna' as established by Wang *et al.* (2011), stretching approximately from 10 to 50 km west of Tuosu Lake in Haixi Mongolian and Tibetan Autonomous Prefecture. The holotype of *Q. cheni*, IVPP *RV37100* (field number No.441), is from the eastern end of the 'General Strips' at point 183, whereas IVPP RV37102 (field number No.508) for *Qurliqnoria* sp. from the same original description is from the western end of the 'General Strips' east of point 42 (see Wang *et al.*, 2011: fig. 7, appendix I).

Age and stratigraphy: Lower part of the Upper Youshashan Formation (Wang *et al.*, 2007), included in the Early-Late Miocene Tuosu Fauna, ~12–10 Mya (Fang *et al.*, 2007) or early Bahean East Asian Neogene Mammal Age (Wang *et al.*, 2008, 2013).

Note on age of Q. cheni *from Wuzhong:* The locality of *Q. cheni* from Wuzhong (described by Qiu *et al.*, 1987) is thought to be correlated with the Ganhegou Formation, which has been estimated using magnetostratigraphic analyses to be 9.26–2.23 Mya (Shen *et al.*, 2001).

However, given the indirect association of these dates (the fossil locality and the palaeomagnetic sections are in different locations), we cautiously interpret the Wuzhong occurrence as possibly younger in age than the *Qurliqnoria* samples from Quanshuiliang.

Description: IVPP V16949 (Fig. 4) is a partial cranium missing the face rostral to the frontals; the right and left horncores are broken ~60 and 80 mm from the base, respectively. Weathered but distinct longitudinal grooves are present on both horncores, but the caudal face has a single deep longitudinal groove ~5 mm wide. The long axis of the horncores in the transverse plane forms an angle of 38° with the sagittal axis, with the rostral ends closer together than the caudal ends. An anterior keel is visible on the right horncore but weathered away on the left. The supraorbital foramina are poorly preserved, but their dorsal rims are located ~29 mm below the anterior face of the horncores. Sinuses are present inside the pedicle, but do not appear to extend into the horncores. Shallow but dorsoventrally expanded postcornual fossae are present and immediately caudal to the caudal wall of the horncore, aligned on its long axis. The left orbital rim is preserved and extends laterally as the outermost
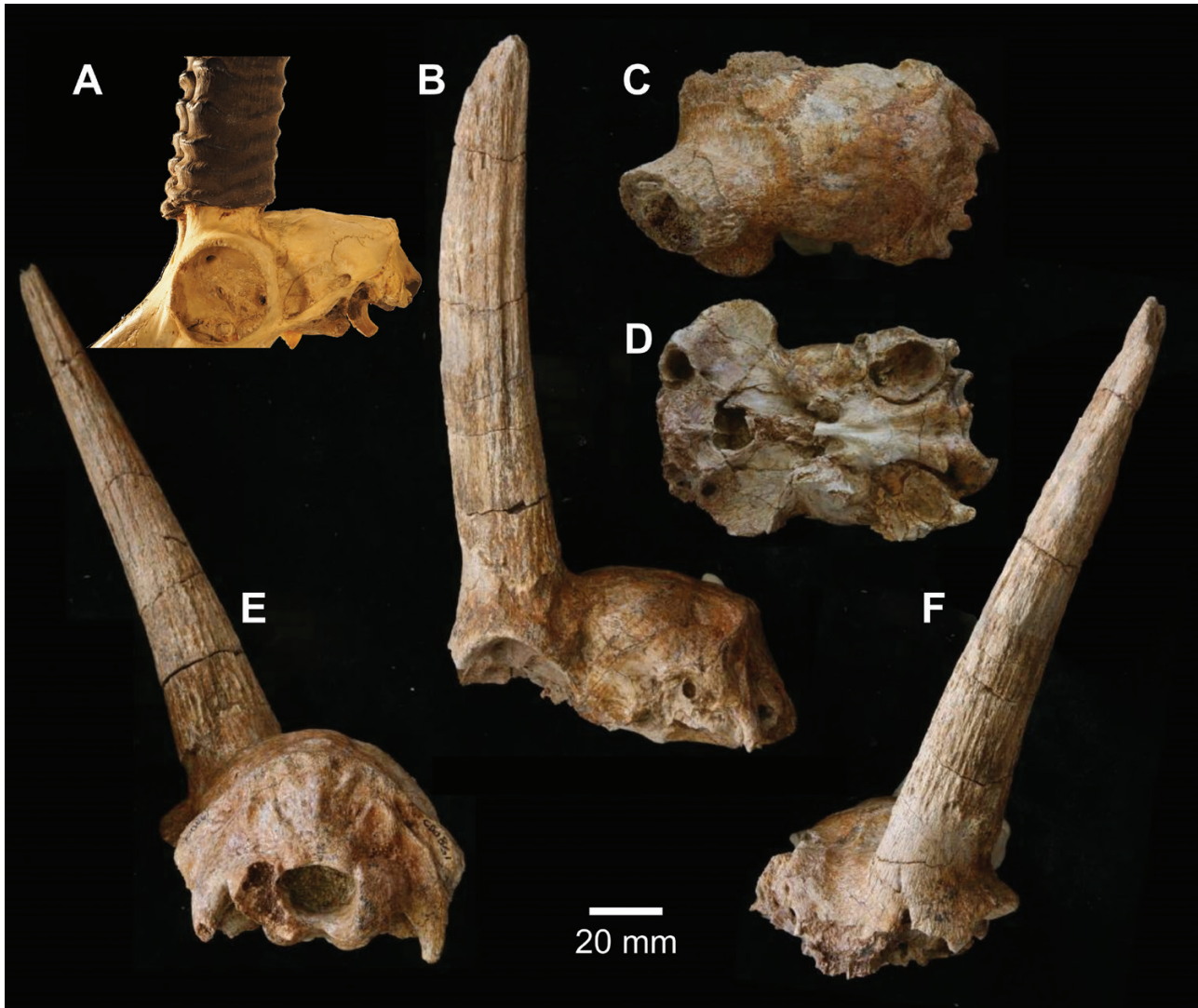
Figure 2. Representative specimens of *Pantholops hodgsonii* (A) and *Qurliqnoria cheni* (B–F) specimens. A, *Pantholops hodgsonii*, NMNH 122758, scaled to same cranium length as the fossil specimen. B-F, *Q. cheni* IVPP V16952 lateral (B), dorsal (C), ventral (D), posterior (E) and anterior (F) views. *Pantholops* photograph by B. Santaella Luna.

feature on the cranium. Viewed laterally, the horncores are inserted at a right angle to the cranial roof, the pedicle being higher rostrally (extending ~30 mm above the frontal bone) than caudally (< 10 mm above the frontal bone). A strong frontoparietal suture is present as a raised ridge, but the interfrontal suture forms a ridge only along the caudal 50% of its length, becoming flat on the cranial roof along the rostral half of the suture between the horncores. The dorsal boundary of the mastoid is in line with the temporal and does not border the parietal. The paroccipital processes are short, but an inflated bulla extends ventrally along its length. The basioccipital has a central groove with a weak mid-sagittal ridge, appearing between the anterior tuberosities and extending rostrally. The

basioccipital is widest at the transversely bulbous posterior tuberosities, becoming restricted a short distance rostrally where the bulla inserts diagonally with its major axis tilting rostromedially; the basioccipital expands again at the transversely bulbous anterior tuberosities. The anterior tuberosities form a triangular area with a rounded caudal-medial corner. A distinct foramen ovale is present, with its long axis oriented dorsocaudally to ventrorostrally. The occipital forms an angle of 128° with the cranial roof.

IVPP V16952 (Fig. 2B–F) is a partial cranium missing the entire region rostral to the frontal bones. The right horncore is not preserved, whereas the left one is almost complete. Cranial features are identical to those in IVPP V16949 except in four aspects. First,
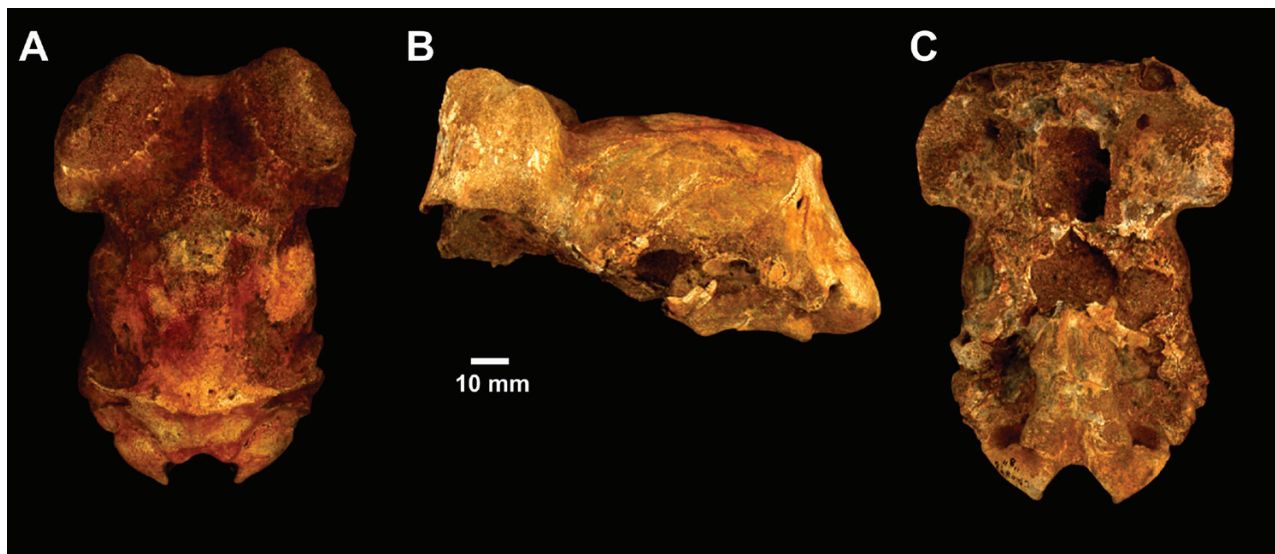
Figure 3. *Qurliqnoria cheni* IVPP V16960. Partial cranium. Dorsal (A), left lateral (B) and ventral (C) views.

there is a small pit present ~6 mm dorsal to each supraorbital foramen, inserted immediately medially to it. Second, two 5-mm-wide longitudinal grooves are present on the left horncore, one originating rostromedially, the other caudolaterally. The grooves become anteroposteriorly oriented near the tip of the horncore, 160 mm from the base, because of the anti-clockwise rotation of the left horncore. Third, the right paroccipital process is almost complete and extends 16 mm ventrolaterally from its base; this process is unlike the shorter ones in IVPP V16949. Fourth, the basioccipital is more quadrate in shape than that in IVPP V16949, with the middle constriction being much less apparent and associated with more circular auditory bullae. The medial ridge is also barely visible in the mid-sagittal groove of the basioccipital, showing only between the anterior tuberosities. Other horncore and cranial specimens show similar morphology to IVPP V16949 and V16952 (Figs 3–6).

The substantial new fossil sample of *Qurliqnoria* provides a firm basis for quantifying intraspecific variation and the first cladistic analysis to place *Qurliqnoria* among extant and fossil bovids. Horncore cross-section dimensions of *Q. cheni* specimens described in the present study overlap with those of extant and fossil *Pantholops* and encompass those of previously described *Qurliqnoria* specimens (Fig. 6). Despite uncertainty in the precise placement of *Qurliqnoria* because of known challenges in using morphological characteristics to classify bovids, cladistic analysis of horncore and cranial characters with varying constraints nevertheless supports a close relationship between *Pantholops* and *Qurliqnoria* (Fig. 7). Dental material tentatively associated with

Qurliqnoria provides additional evidence that the fossil bovid lies near the base of the Caprini–*Pantholops* clade (Figs 8–14).

Comparison of horncores with other bovids: As early as 1968, Alan Gentry pointed out the similarity in horncore morphology between *Q. cheni* and the extant *Pantholops hodgsonii* (Fig. 5B, C): strong lateral compression at the distal region of the horncores, the presence of anterior keels, stronger longitudinal grooves on the posterior part of the horncores, upright insertion of the horncores on the skull and little backward curvature distally, short pedicel, closely set supraorbital foramina, which are simple pits, and potentially wide orbital rims (this part of the anatomy was poorly preserved among Bohlin's available materials) (Gentry, 1968). All these observations are still valid, and the new materials described here provide strong support for the comparisons Gentry made more than five decades ago (Figs 2, 4). The two differences Gentry (1968) cited, the larger size of *Qurliqnoria* and the more raised frontals of the fossil form, are maintained, but the latter difference is small. The mid-frontal suture in *Qurliqnoria* is raised only in the caudal 50% toward the frontoparietal suture; the suture flattens out rostrally, and although still visible, the suture is not raised as a ridge.

The holotype specimen IVPP *RV37100* that Bohlin (1937) designated to *Q. cheni* and IVPP RV37102 for *Qurliqnoria* sp. is consistent in morphology and size with the new materials described in the present study and with extant *Pantholops* (Tables 2 and 3). The divergent horncore tips in the better-preserved new Qaidam specimens are similar to those in the
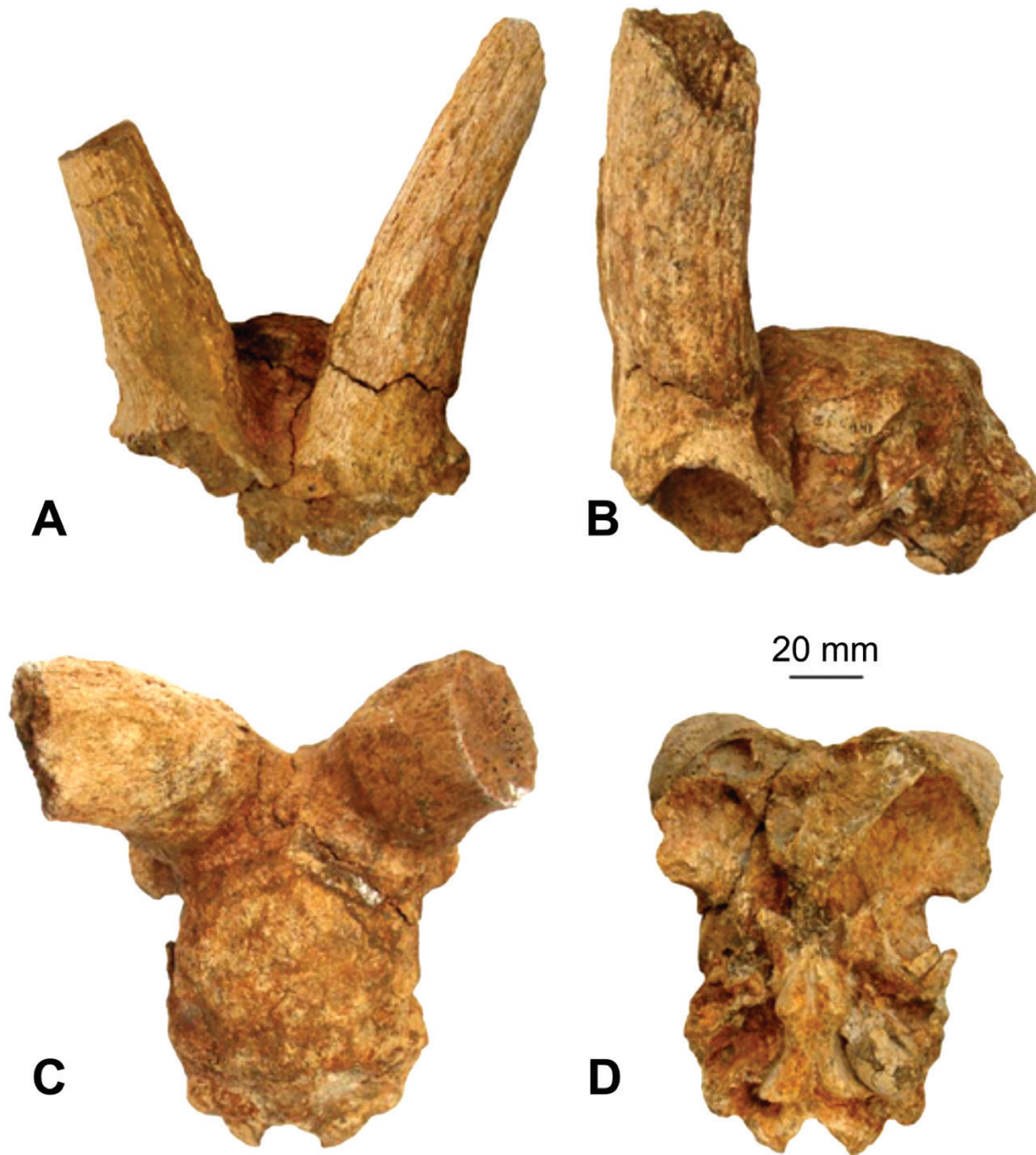
Figure 4. *Qurliqnoria cheni* IVPP V16949. Partial cranium with partial horncores. Rostral (A), left lateral (B), dorsal (C) and ventral (D) views.

holotypes figured by Bohlin (1937: plates III.6 and IV.2 #740). The increased sample size provided by the more recent collections in the Quanshuiliang area shows a wider range of sizes and morphological variation than was known by Bohlin (1937); thus, the specimen he separated out from *Q. cheni* as *Qurliqnoria* sp. (IVPP RV37102) is now considered to be *Q. cheni*, its horncore dimensions being within the variational range of the species (Table 3; Fig. 6). In our new sample, the longitudinal grooves on the horncores of *Q. cheni* are more distinct on the larger specimens and less so on the smaller ones; even after

accounting for differential weathering, the horncore sample still clearly shows the difference described above. However, the absolute sizes of the horncores do not cluster by this morphological difference; the horncores range continuously in size (other than a small gap at ~38 mm anteroposterior length) from 34.4 mm × 22.2 mm to 47.3 mm × 30.6 mm. See the section on intraspecific variation for a discussion of possible sexual dimorphism or an ontogenetic series.

Qiu *et al.* (1987) referred a pair of partial horncores from Wuzhong County in Ningxia Province to *Q. cheni*, and they used these specimens to infer an age of

Table 2. Skull and horncore measurements of *Qurliqnoria cheni*

Measurement	IVPP	IVPP	Bohlin (1937)	
	V16952	V16949	IVPP *RV37100*	IVPP RV37102
DT of horncore base	25.7	27.3,27.3	30.0	28.0
DL of horncore base	37.7	44.1,44.3	48.0	40.0
Width across pedicles	[80]	86.5	88.0	88.0
Width between pedicles	18.7	13.0	14.0	17.0
Length of horncore	160+	–	203+	–
Width at supraorbital pits	36.0	26.1	31.0	34.0
Width of braincase	66.3	69.0	–	–
Skull width at orbits	[96]	[100]	100.0	–
Height of foramen magnum	14.0	16.6	–	–
DT of foramen magnum	20.0	17.0	–	–
Width across condyles	44.7	44.7	–	–
Height of occiput	30.7	31.4	–	–
Width across mastoids	75.7	75.3	–	–
Width of anterior basioccipital	23.3	20.3	–	–
Width of posterior basioccipital	28.6	32.1	–	–
Length of auditory bulla	27.6	28.9	–	–

Values in brackets are estimated. All measurements are in millimetres. Abbreviations: DL, long-axis distance; DT, transverse distance.

middle Bahean for the Wuzhong local fauna based on their assessment of the biochronology. In addition to horncore dimensions (43 mm × 26.5 mm in maximum cross-sectional measurements), which fall within the range of variation observed in the Quanshuiliang sample of *Qurliqnoria*, the anteromedially slanted orientation of the horncore bases and the presence of a clockwise rotation of the right horncore prompted their assignment of the specimen to *Q. cheni*. The Ningxia specimen is fragmentary, but lacking any diagnostic characteristics to the contrary, we follow that designation here as the only Chinese locality outside of Tibetan Plateau with the occurrence of *Qurliqnoria*.

Ozansoy (1957) named a new species of *Qurliqnoria*, *Qurliqnoria senyureki* Ozansoy, 1957, from the middle Sinap Formation in Turkey; among the contemporaneous bovid elements of that fauna are *Protoryx carolinae* Major, 1891 and *Protoryx* (*Pachytragus*) *longiceps* Pilgrim & Hopwood, 1928. Given that Ozansoy provided no adequate description of the species of *Qurliqnoria* he named and that subsequent works on Sinap bovids have not recovered additional material of *Qurliqnoria* (Ozansoy, 1958; Gentry, 2003; Sen, 2003), we tentatively declare *Q. senyureki* a *nomen nudum*, until fossil discoveries demonstrate otherwise.

Azanza & Morales (1994) reviewed the European, African and Indian fossils previously associated with *Caprotragoides* Thenius, 1979, and established two new genera, *Tethytragus* and *Gentrytragus* Azanza & Morales, 1994, to the European and African–Middle

Eastern taxa, respectively. The genotype species of *Tethytragus* is *Tethytragus langai* Azanza & Morales, 1994, with the type locality at Arroyo Val-Barranca in Spain. The holotype specimen *BAR-73* is a pair of horncores with partial frontals; the horncore is smaller than those of *Qurliqnoria*, but they have a few morphological similarities. The strong anterior and posterior grooves are present on both, in addition to shallower grooves throughout the surface of the horncores. The horncores in both taxa have a long axis that tilts toward the sagittal axis rostrally, and both have upright insertions of the horncore on the cranial roof. Both taxa also share a lack of raised interfrontal suture between the horncores. Both taxa have sinuses in the pedicle of the horncore that do not extend into the horncore itself. *Qurliqnoria cheni* shares the presence of postcornual fossa with *Tethytragus langai* from Paracuellos 3 locality of Spain and with *Tethytragus koehlerae* Azanza & Morales, 1994 from Paşalar, Turkey (Gentry, 1990).

Protoryx carolinae from the Pikermi *Hipparion* fauna represents a basal caprin or hippotragin with laterally compressed and caudally curved horncores; rotation of the horncores is essentially non-existent, differing from the horncores of *Qurliqnoria*, which show gradual but continuous rotation (homonymous) beginning at the base immediately above the pedicle. The arrangement of the cross-section long axes of the horncores is also close to parallel in *Protoryx*, whereas in *Qurliqnoria* the horncore cross-section long axes converge toward each other rostrally. The orientation of the horns in two *Pantholops* specimens (NMNH

Table 3. Horncore measurements of *Qurliqnoria cheni* compared with extant *Pantholops hodgsonii* (NMNH specimens)

Locality	Specimen	Side	DL	DT	DT/DL
CD2001.8.10	IVPP V16942	Right	47.3	30.6	0.65
CD2001.8.10	IVPP V16942	Left	46.8	28.9	0.62
CD0776	IVPP V16943	Right	34.4	22.2	0.65
CD0793	IVPP V16944	Right	36.2	23.6	0.65
CD0808	IVPP V16946	Left	36.6	26.6	0.73
CD08101	IVPP V16962	Right	35.0	23.7	0.68
CD08118	IVPP V16963	Left	42.6	30.2	0.71
CD08123	IVPP V16964	Right	46.0	31.8	0.69
CD0833	IVPP V16947	Left	39.3	22.5	0.57
CD0835	IVPP V16948	Left	43.9	29.1	0.66
CD0841	IVPP V16949	Right	45.0	28.1	0.62
CD0841	IVPP V16949	Left	44.8	27.7	0.62
CD0851	IVPP V16950	Left	39.3	28.0	0.71
CD0860	IVPP V16951	Right	36.5	22.6	0.62
CD0861	IVPP V16952	Left	36.4	25.7	0.71
CD0864	IVPP V16953	Right	41.6	29.3	0.70
CD0865	IVPP V16955	Left	41.6	26.1	0.63
CD0876	IVPP V16957	Right	41.8	27.3	0.65
CD0880	IVPP V16958	Right	45.6	29.6	0.65
CD0896a	IVPP V16959	Right	45.0	32.8	0.73
CD0896a	IVPP V16959	Left	44.3	30.2	0.68
CD0896b	IVPP V16960	Right	40.5	30.2	0.75
CD0896b	IVPP V16960	Left	40.5	28.9	0.71
CD9824	IVPP V16941	Right	36.9	25.1	0.68
Qiu *et al.* (1987)	IVPP V7164	Both	43.0	26.5	0.62
Bohlin (1937)	IVPP *RV37100*	Both	48.0	30.0	0.63
Bohlin (1937)	IVPP RV37102	Both	40.0	28.0	0.70
–	NMNH 122758	Right	42	30	0.71
–	NMNH 122758	Left	39	29	0.74
–	NMNH 20833	Right	46	28	0.61
–	NMNH 20833	Left	48	27	0.56

All measurements are in millimetres. Abbreviations: DL, cross-section long-axis distance; DT, transverse distance.

122758 and 20833) appears to show a similar rostral convergence between the cross-section long axes, but the orientation of the horncores could not be verified because they were obscured by the overlying horn sheath. The curvature of the horncores is more extreme in *Protoryx* (Pilgrim & Hopwood, 1928), with the distal ends of horns reaching caudally significantly further than in *Qurliqnoria*. In this regard, the curvature of *Protoryx* is similar to that of another Qaidam Basin bovid, *Olonbulukia tsaidamensis* (Bohlin, 1937). The presence of complicated sutures between the frontals at the position between the horncores in *Protoryx carolinae* is not seen in *Qurliqnoria*, where the suture begins as a raised ridge with winding patterns but merges smoothly into a flat 'forehead' halfway in between the horncore pedicles. Bohlin (1937) mentioned the strong fusion of the frontal in between the horncores in his description of the

holotype of *Qurliqnoria* and gave it as the reason for the preservation of the paired horncores he described.

Two *Protoryx* species, *Protoryx enanus* Köhler, 1987 from MN7 of Turkey and *Protoryx solignaci* (Robinson, 1972) from MN8/9 of Tunisia and Turkey, are geologically older than all other *Protoryx* taxa, but are not unambiguously plesiomorphic in their morphological characteristics (Gentry, 2000). Unlike *Qurliqnoria*, *Protoryx enanus* has no internal sinus in the pedicle, but both taxa have closely set supraorbital foramina and lack of a raised ridge on the interfrontal suture (Köhler, 1987). Horncores with an anterior keel and presence of a postcornual fossa are features shared by *Protoryx solignaci* and *Q. cheni* (Gentry, 2000). Lacking clear autapomorphic features in this regard, *Q. cheni* could be related to the basal members of the *Protoryx* group by common features on their horncores and cranium.
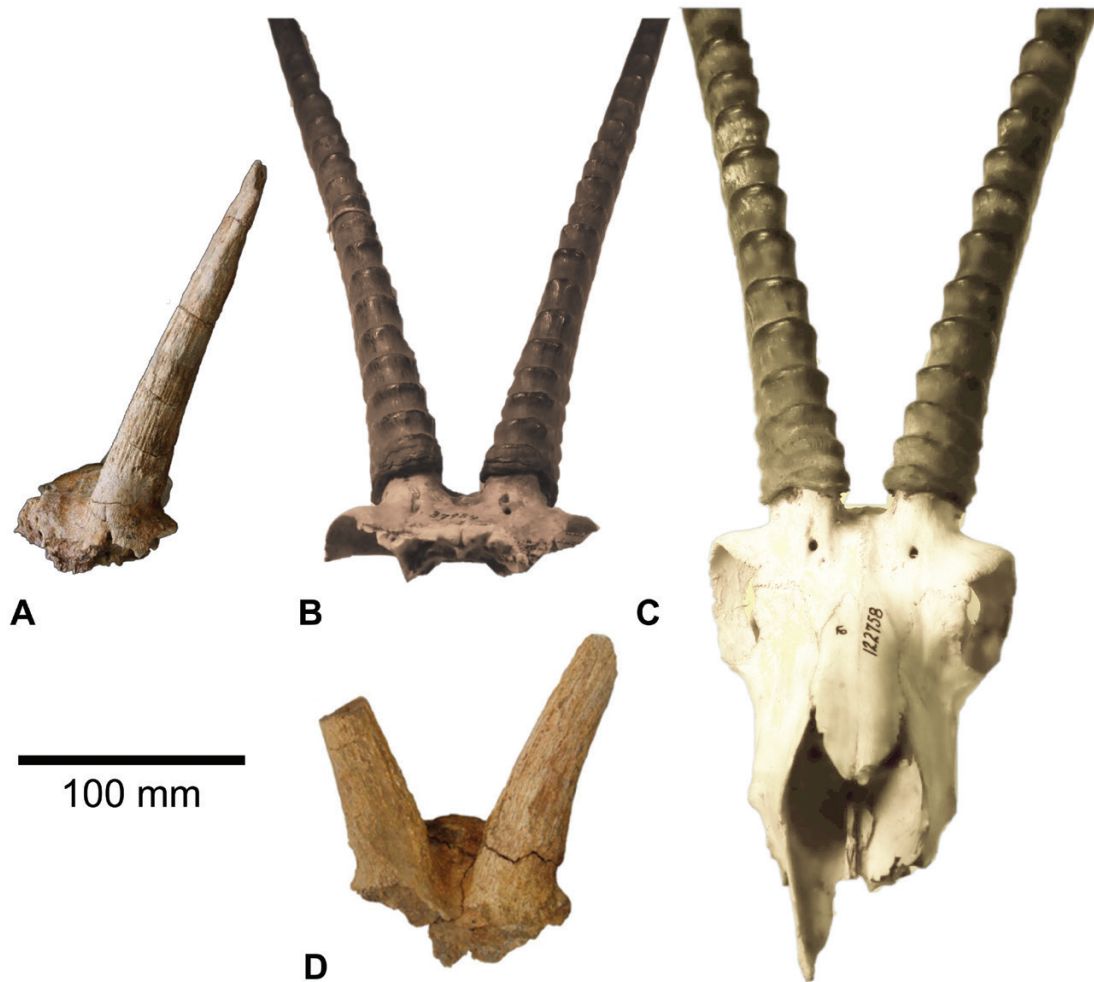
Figure 5. Comparison of *Qurliqnoria* horncores and *Pantholops* horns. A, *Qurliqnoria cheni* IVPP V16952 rostral view. B, *Pantholops hodgsonii* NMNH 20833 rostral view. C, *P. hodgsonii* NMNH 122758 rostral view. D, *Q. cheni* IVPP V16949 rostral view.

Pachytragus has a more curved horncore profile, as in *Protoryx* but unlike *Qurliqnoria*. In *Pachytragus*, the basioccipital has elongate and sagittally oriented anterior tuberosities, whereas *Qurliqnoria* has more transversely bulging anterior tuberosities that taper off anteriorly. *Pachytragus* lacks postcornual fossae, whereas they are present in *Qurliqnoria*. Furthermore, there is no visible rotation of the horncores in *Pachytragus*, but moderate rotation in *Qurliqnoria*. The occipital and cranial roof of *Pachytragus crassicornis* Schlosser, 1904 from Akkaşdaği, Turkey (Kostopoulos, 2005) are at an angle of 115° to each other, whereas in *Qurliqnoria* (IVPP V16949 and V16952) the angle is 128°. This is representative of the fact that the cranial roof in *Pachytragus crassicornis* is relatively flat, whereas in *Qurliqnoria* it is bulging in the parietal and interparietal bones, although such differences might also be within measurement error.

The length of the horncore in the holotype (IVPP *RV37100*) of *Q. cheni* is ~203 mm (Bohlin, 1937), shorter than the 280 mm horncore on *Pachytragus crassicornis* from Akkaşdaği (Kostopoulos, 2005). The horncores are inserted on the frontals at 90° to the cranial roof in *Q. cheni*, not tilting backward as in *Pachytragus crassicornis* (Kostopoulos, 2005). The long axis of the horncores forms an angle between 34 and 38° in *Q. cheni*, less parallel than the 25° angle observed in *Pachytragus crassicornis* (Kostopoulos, 2005). The basioccipital bone in *Q. cheni* can be more triangular than in *Pachytragus crassicornis*, which is, in turn, more triangular than in *Protoryx carolinae* (Kostopoulos, 2005). *Qurliqnoria cheni* also differs in having a constriction of the basioccipital bone between the anterior and posterior tuberosities, making the sides concave and not as straight as in *Pachytragus crassicornis*. These comparisons between *Qurliqnoria*
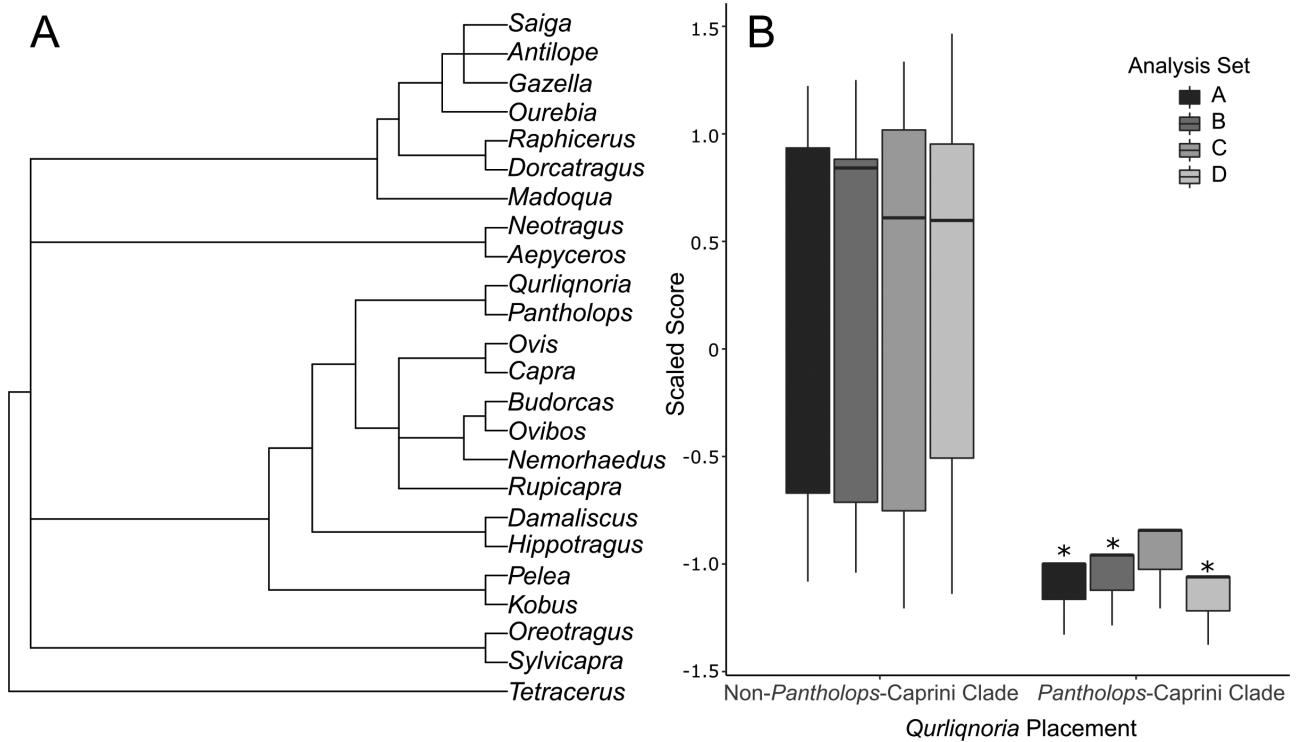
Figure 6. Scatterplot and *k*-means cluster analysis of the horncore cross-section long-axis length vs. transverse width measurements of *Qurliqnoria cheni* specimens. A, bivariate plot of specimens from Qaidam Basin described in the present study (filled circles), *Q. cheni* IVPP *RV37100* (grey square), IVPP RV37102 (orange square), IVPP V7164 from Wuzhong (open circle), extant *Pantholops hodgsonii* (triangles) and fossil *Pantholops hundesiensis* (green diamond). B, plot of clusters identified using the silhouette method on *k*-means cluster analysis results. Cluster 1 represents larger specimens and cluster 2, smaller specimens.

and *Protoryx–Pachytragus* indicate a group of genera with shared morphological features, but the former exhibits more plesiomorphic cranial features, such as a flat interfrontal suture, compared with geologically younger members of the latter group. These taxa could be basal to crown group caprins (Solounias & Moelleken, 1992; Gentry, 2000).

The basal caprin *Protoryx* includes several species in China originally described by Bohlin (1935b) and Teilhard de Chardin & Trassaert (1938), which were subsequently placed into two endemic Chinese genera, *Huabeitragus* and *Macrotragus*, by Chen & Zhang (2007). *Huabeitragus yushensis* (Teilhard de Chardin & Trassaert, 1938) from the Pliocene Yushe Basin of northern China has more widely spaced supraorbital foramina relative to the outer width of the horncore bases than in *Q. cheni*. In neither genus does the mastoid contact the parietal. The basioccipital in *Huabeitragus* is square in outline and lacks longitudinal ridges posterior to the anterior tuberosities, which are strong in *Qurliqnoria* and followed by posteriorly diverging ridges. The divergence of the horncore tip in *Huabeitragus* is to a more extreme extent than in *Qurliqnoria*. Both possess anterior keels on horncores.

Macrotragus from Shanxi and Gansu Provinces has a similar triangular basioccipital to *Qurliqnoria*, but an example of *Macrotragus shansiensis* (Bohlin, 1935) from Baode (IVPP V14755) shows the presence of a strong mid-sagittal ridge on the basioccipital anterior to the anterior tuberosities, which is not

observed in *Qurliqnoria*. The suture between the frontals at the position of the horncores appears to be rugose and unfused in *M. shansiensis*, whereas in *Qurliqnoria* the suture is hardly visible and does not rise as a ridge between the horncores. The cranial axis dips down dramatically in *Macrotragus* at the position of the horncores, whereas in *Qurliqnoria* there is only a slight dip (< 45°) downward between the horncore bases.

Chen (2005) described a new species of *Dorcadoryx*, a medium-sized bovid with transversely compressed horncores similar to those of *Protoryx*. She cited several differences between *Dorcadoryx* and *Protoryx–Pachytragus*, such as the lack of a raised interfrontal ridge between the horncores and the fusion of the p4 paraconid and metaconid in the former. Among the characters that differentiate *Qurliqnoria* from *Dorcadoryx*, there is the lack of horncore rotation, the lack of lateral expansion of the orbit, and a much smaller radius of curvature of the horncore in the latter. Chen (2005) referred the material previously identified as *?Tragoreas* from China and Mongolia to *Dorcadoryx*, and suggested that *Qurliqnoria* might belong in the same group. Based on the available material, there are enough morphological features (such as a triangular occipital, transversely compressed horncores and presence of an anterior keel on horncores) to link *Qurliqnoria* with the Chinese *Dorcadoryx*, *Huabeitragus* and *Macrotragus*, which share morphological characteristics with the

Figure 7. Cladistic analyses. A, the most parsimonious morphological phylogeny using 112 characters from Gentry (1992). Only horncore and skull characters were coded for *Qurliqnoria*. Mitochondrial DNA backbone constraint from Bibi (2013), with only monophyly of tribes enforced (topology within tribes unconstrained), and with *Qurliqnoria* within a Caprini + *Pantholops* clade. B, comparison of scaled tree scores across all analysis sets between constraints that place *Qurliqnoria* within a *Pantholops*–Caprini clade vs. those that do not. Asterisks indicate Kruskal–Wallis test statistic for tree score differences at $P < 0.05$. For tree scores and additional sensitivity analyses, see main text and Table 1.

Protoryx–Pachytragus lineage. However, the resolution of the interrelationships among the Chinese forms and between the Asian and European forms requires a more thorough examination of the morphologies and cladistics of the group.

Intraspecific variation in Qurliqnoria *horncores:* As mentioned above, the extent of longitudinal grooving is associated with the size of individuals from Quanshuiliang. Larger individuals tend to have deeper and distinct longitudinal grooves, whereas smaller individuals have shallower grooves that are more easily obliterated by post-mortem weathering. We examined the distribution of horncore dimensions on a scattergram, and there is no clear division between the two morphotypes based on horncore dimensions (Fig. 6A). However, the bivariate scattergram does suggest clustering in the distribution, into specimens with horncore lengths < 38–39 mm vs. those with lengths > 39 mm. The outlying specimen at 39.3 mm × 22.5 mm (IVPP V16947) appears to be a weathered specimen, which is not representative of its original dimensions. Thus, this gap in horncore size might indicate a bimodal

distribution. An analysis of the optimal number of clusters using the silhouette method on k-means-clustered data (done using the *factoextra* package in the R programming environment; Kassambara & Mundt, 2020) supports the interpretation of two clusters in the horncore data (Fig. 6B). Nevertheless, the range of horncore sizes observed in the sample of Qaidam *Qurliqnoria* is no larger than those found for other Late Miocene bovids (Kostopoulos, 2005; Bibi & Güleç, 2008); the fossil sample analysed here ($N = 20$) could be too small and/or too time averaged to provide strong evidence of sexual dimorphism if it exists. If additional specimens fail to fill in this gap in horncore size, a case for sexual dimorphism will be strengthened. Alternatively, a continuous distribution of horncore sizes across the observed range might indicate the presence of an ontogenetic series of subadult to adult individuals in the Quanshuiliang *Q. cheni* sample or a variable adult population. Horned females, if present, would be a derived trait that evolved in *Qurliqnoria*, which is not shared with *Tethytragus* (Geraads, 2003), *Pantholops* (Leslie & Schaller, 2008) or, questionably, *Pachytragus* (Gentry, 1971).

Despite morphological similarity (Figs 4, 5) and close phylogenetic affinity (Fig. 7; see 'Cladistic analysis' in the Results section), there remains a maximum 6 Myr time gap between the Early and Late Miocene *Qurliqnoria* and *Pantholops*, with the latter having its earliest record in Pliocene deposits in Tibet as *Pantholops hundesiensis* Lydekker, 1881 Lydekker (1901) (Wang *et al.*, 2020). The type specimen of *Pantholops hundesiensis* (Natural History Museum London NHMUK M10888) preserves only a fragmentary base of one horncore on top of a cranial specimen and provides little information for comparison with the *Qurliqnoria* materials described here. Our field expeditions in the western Tibet Mio-Pliocene Zanda Basin produced two horncore specimens possibly representing *Pantholops* (Fig. 1). One of the specimens (undescribed, from field locality ZD0904, Early Pliocene) is a partial horncore fragment, broken proximally at the base of the pedestal and distally ~95 mm from the top of the pedestal. The shape of the cross-section is oval, with an anteriorly tapering edge, which corresponds to the strong keel running on the anterior face of the horncore. The horncore lacks the strong grooving that is present in *Qurliqnoria*, but several short channels are present on the posterior face of the horncore extending from nutrient foramina. There is a clear trench circumventing the base of the horncore at the pedestal, but there is no constriction of the pedestal, which has about the same girth as the horncore. This condition is similar to the morphology observed in a horncore of the extant *Pantholops hodgsonii* collected by us on the Kunlun Mountain Pass in Qinghai Province. At the base of the horncore where it is broken, a strong upward-extending chamber of the frontal sinus is present, forming an elongated space ending dorsally at the pedestal–horncore trench. This specimen suggests a possible range extension for *Pantholops* beyond its present geographical distribution (Fig. 1). Another specimen, from the Zanda locality ZD0745 (Deng *et al.*, 2011: supplementary material fig. 2, Early Pliocene), was preliminarily identified as *Qurliqnoria* by Deng *et al.* (2011). The smoother horncore surface on this specimen than on the Qaidam specimens described herein, despite the relatively large size of the former, is consistent with *Pantholops*. Further fieldwork to discover more complete fossils in the Zanda Basin and in the Kunlun Pass Basin (Li *et al.*, 2014) is necessary to clarify whether *Qurliqnoria* and *Pantholops* overlapped stratigraphically or potentially represent a single anagenetic lineage.

CF. *QURLIQNORIA CHENI*
(FIGS 8–12; TABLE 4)

Referred material: IVPP V16945, partial left dentary with Lm1–m3, from the CD07106 locality; IVPP
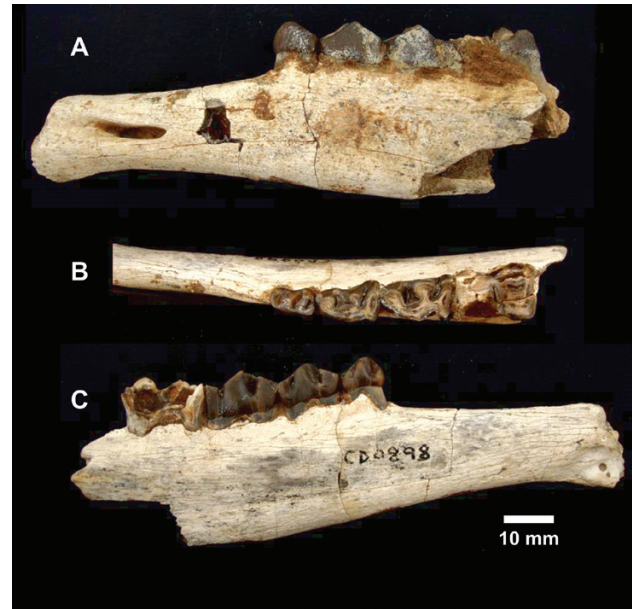

Figure 8. cf. *Qurliqnoria cheni* IVPP V16961. Partial left dentary with p4–m1. Lateral (A), occlusal (B) and medial (C) views.

V16954, partial left dentary with Lp4–m3, from the CD0864 locality, collected by Jack Tseng on 2 September 2008; IVPP V16956, partial left dentary with Lp3, Ldp4 and Lm1, from the CD0869 locality, collected by Min Zhao and Xiaoming Wang on 2 September 2008; and IVPP V16961, partial left dentary with Lp2–m1, from the CD0898 locality, collected by Qiang Li on 6 September 2008.

Localities, stratigraphy and age: Same as those described in the preceding section on the systematic palaeontology of the horncore specimens.

Description: IVPP V16961 (Fig. 8) is a left partial mandible with p2–p4, partial m1. The p2 is four-lophed; the protoconid is the largest cusp, least worn; the parastylid is simple, and points anterolingually; the entoconid and entostylid do not contact each other on the lingual side, and the valley between them is open for the most part except at the base. The p3 paraconid and parastylid are fused from wear; a short, circular and bulbous metaconid extends posterolingually from the protoconid; the hypoconid is more columnar labially than in p2; and the entoconid and entostylid connect at the lingual side to form a central cavity. There is a clear indentation labially between the protoconid and hypoconid. The p4 parastylid and paraconid are fused; the metaconid and protoconid are worn to roughly same size, with the metaconid situated posterolingually of the protoconid; the entoconid and entostylid are completely fused, with the central cavity not visible; the hypoconid
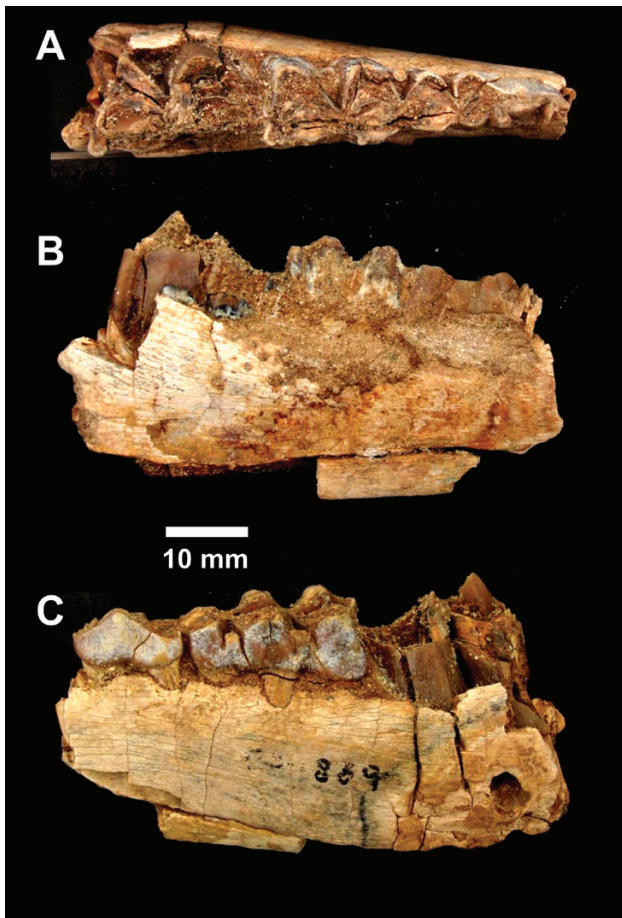
Figure 9. cf. *Qurliqnoria cheni* IVPP V16956. Partial left dentary with p3, dp4 and m1. Occlusal (A), lingual (B) and labial (C) views.

is large and points posterolabially, and the labial valley between the hypoconid and protoconid is deep and distinct. The m1 anterior loph is incomplete; the hypoconid is worn to large lake, with a small central cavity; and the lingual side is incomplete. It is unclear whether a basal pillar is present.

IVPP V16956 (Fig. 9) is a left partial mandible with p3–dp4, partial m1. Left p3: anterolingual side broken, with parastylid and paraconid incomplete; the metaconid is distinct but smaller than the protoconid; the entoconid and entostylid are fused, with the central cavity oriented diagonally toward the posterolingual corner; and the hypoconid is worn, with the labial wall bulging. Left dp4: three-lophed, with anterior loph simple, middle loph with distinct entostylid, and two basal pillars in labial valleys. Left m1: incomplete, with two cracked lophs.

IVPP V16954 (Fig. 10) is a partial right dentary with partial p4 and m1–m3. The anterior loph of p4 is missing, leaving only the posterior half of the tooth, beginning with the protoconid and metaconid. The

labial side of p4 is also broken, hence the degree of labial valley development immediately anterior to the hypoconid cannot be discerned. The metaconid and entoconid are not fused. Small basal pillars are present on m1–m3. The lingual walls of the molars are slightly convex between the stylid cusps, and a 'goat fold' (Gentry, 1992) is absent on m3; the analogous position on m1~m2 is broken.

IVPP V16945 (Fig. 11) is a partial left dentary, with broken m1 and moderately worn m2 and m3. The dental morphology is similar to that in V16954. Small basal pillars are present on m2–m3. The lingual walls of m2 and m3 are gently convex between the stylid cusps. Goat folds are absent on m2–m3; m1 is too incomplete to observe this feature.

Comparison: We pooled all measurable horncore specimens of the Qaidam Basin expedition 1998–2008 and obtained the following relative abundances: *Q. cheni* (20 specimens), *?Gazella* sp. (18), *Olonbulukia tsaidamensis* (3) and *Tossunnoria pseudibex* (2). During the same period, eight partial mandibular fragments were collected, four of which were small and low crowned, probably belonging to cervids (specimens of which are the subject of a separate study). The remaining four partial dentaries represent a bovid taxon that is consistent with the morphology represented by the horncores and crania of *Q. cheni* described in the previous section when compared with more complete specimens of other fossil bovids, such as *Protoryx* or *Pachytragus*. For example, the slightly shortened premolar row (Fig. 13), diminutive basal pillars on lower molars and a posterior position of the p4 metaconid relative to the protoconid are all characteristics shared by the Quanshuiliang mandible specimens with caprins and their basal relative, *Pachytragus* (Gentry, 2000). Given that a direct association of the horncore/cranium and dentition is lacking for the entire bovid collection from the Qaidam Basin and the Tibetan Plateau as a whole, we refer these dental specimens to cf. *Q. cheni* pending future discovery of more complete material to confirm or falsify our tentative association.

The basal bovid *Tethytragus* has been hypothesized to be ancestral to the *Protoryx–Pachytragus* group, which might have given rise to the crown caprins (Gentry, 2000). The relative length of the premolar toothrow to overall cheek dentition length in a sample of *Tethytragus koehlerae* from Çandir, Turkey is ~67–68% (Geraads, 2003), showing less relative premolar reduction in comparison to the presently referred sample of *Qurliqnoria* (~60.8%) (Fig. 13). The p4 of *Tethytragus koehlerae* (MTA 5107) illustrated by Geraads (2003) shows a labial origin of the metaconid transversely adjacent to the protoconid, not the posterolingual origin seen in *Qurliqnoria*, with the latter suggested to be a more derived trait (Gentry, 1992, 2000). *Tethytragus*
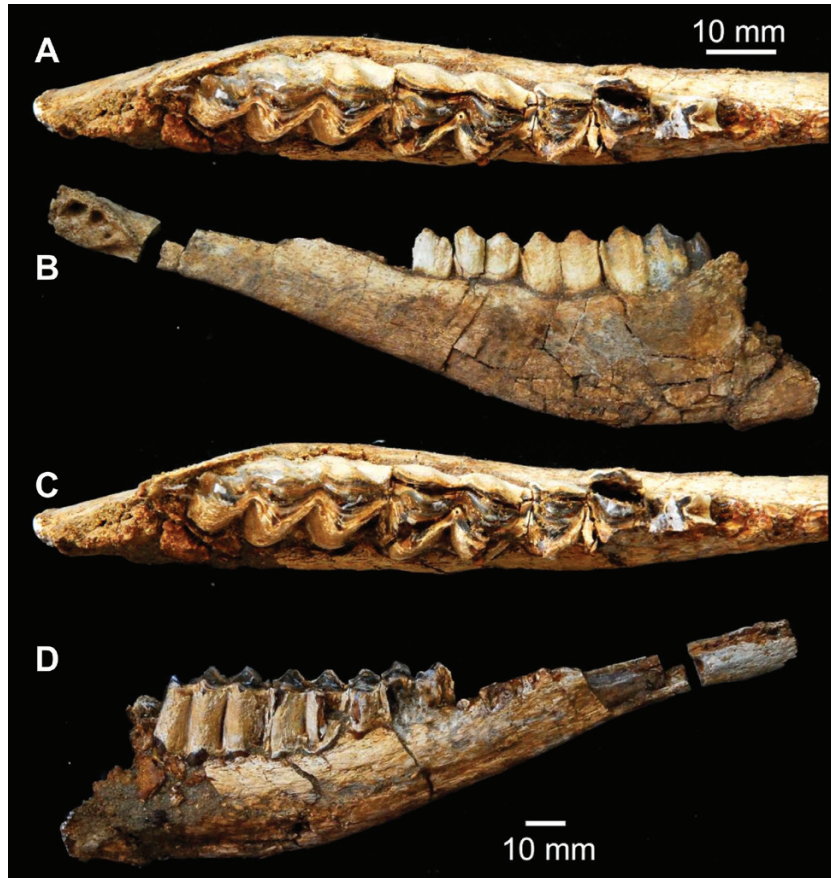
Figure 10. cf. *Qurliqnoria cheni* IVPP V16954. Partial right dentary with partial p4, m1–m3. A, C, stereopair occlusal views. B, medial view. D, lateral view. Top scale bar is for stereopair, bottom scale bar for others.

koehlerae specimens from Paşalar (Gentry, 1990) have smaller lower teeth than *Qurliqnoria*, but the difference is largest in m3 lengths.

The mandible of *Tethytragus langai* (BAR-4) from the Arroyo de Val-Barranca in Spain, figured by Azanza & Morales (1994), shows premolar morphology broadly consistent with that observed in *Qurliqnoria*. The metaconid in p3 and p4 leans posteriorly such that there is a lingual valley between this cusp and the paraconid. The p4 metaconid also appears more bulbous than the p3 metaconid, and the entoconid and entostylid probably fuse in later stages of wear. The *Tethytragus langai* specimen figured by Azanza & Morales (1994) has a moderately worn dentition, whereas the premolars in IVPP V16961 are more heavily worn, obscuring the contact relationships among the cusps and presenting difficulty in direct comparison of the two dentitions.

Based on a conservative estimate of relative premolar-to-molar ratio using IVPP V16945, V16954 and V16961, the premolar toothrow is ~60.8% of the molar toothrow length. This percentage represents a reduced premolar toothrow when compared with other Late Miocene bovids and shows similarity to the *Protoryx–Pachytragus* lineage (Bibi & Güleç, 2008). The premolars of IVPP V16961 and molars of IVPP V16945 and V16954 are all smaller than *?Protoryx* from Sivas (Bibi & Güleç, 2008), and, in particular, the p2 in the former is more reduced. As in the juvenile specimen from Sivas, the left dp4 on IVPP V16956 has moderately developed basal pillars (ectostylids), but the basal pillars on the molars of IVPP V16945 and V16954 are more reduced than those in *?Protoryx* from Sivas.

The estimated length of the lower toothrow of *Qurliqnoria* is shorter than that of *Pachytragus crassicornis* (Kostopoulos, 2005), making the former also smaller than *Protoryx carolinae* (Table 4). The length of the premolar toothrow of *Qurliqnoria* is about the same as in *Pachytragus crassicornis* from Akkaşdaği, but the length of the molar toothrow is shorter in the former. This makes the premolar dentition in *Qurliqnoria* relatively longer than in *Pachytragus* and thus less derived than the
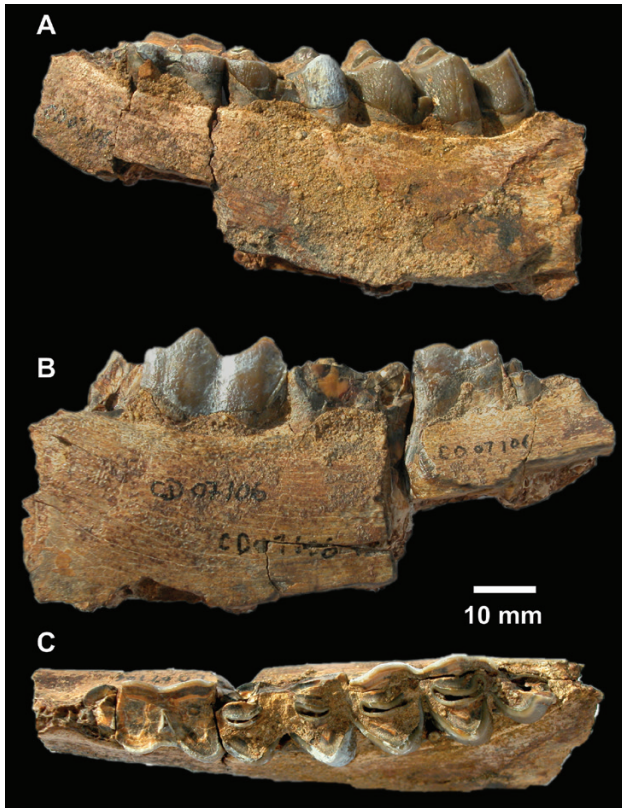
Figure 11. cf. *Qurliqnoria cheni* IVPP V16945. Partial left dentary with m1–m3. Labial (A), lingual (B) and occlusal (C) views.

Pachytragus–Protoryx group. However, based on dental morphology, there are many similarities between the forms: a pointed p4 hypoconid giving the appearance of a large indentation valley immediately anterior to the cusp labially, a bulbous p4 metaconid with wear, and no fusion of p4 paraconid and metaconid, leaving a wide anterolingual valley (Gentry, 1971). Based on these morphological considerations, *Qurliqnoria* displays a suite of morphological characteristics intermediate between *Tethytragus–Gentrytragus* and *Pachytragus–Protoryx* (Fig. 12), suggesting a possible evolutionary position slightly outside the Caprini clade (formerly Caprinae; *sensu* Gentry, 2000), where the extant *Pantholops* lies (see 'Cladistic analysis' in the Results section; Vrba & Schaller, 2000).

RESULTS

CLADISTIC ANALYSIS

Horncores and crania

The most parsimonious tree in phylogenetic analyses of skull and horncore morphology (analysis set A, 23

extant taxa plus *Qurliqnoria*; and set B, set A plus 12 additional fossil taxa) includes *Pantholops* and *Qurliqnoria* in the same monophyletic groups (Table 1; Fig. 7A). Constraints that limited *Qurliqnoria* to grouping with clades other than *Pantholops* + Caprini returned trees with a higher number of steps across the board than those analyses enforcing a *Pantholops* + Caprini constraint for *Qurliqnoria* (Fig. 7B).

Among the cranial and horncore characters from the study by Gentry (1992) available for coding in *Qurliqnoria* (35 of 54 or 65%), *Pantholops* and *Qurliqnoria* share the following synapomorphies (supported by analyses A3–A5 and B3–B5): horncores with keels present [Gentry's character 4(1)]; basioccipital with weak anterior tuberosities [Gentry's character 46(0)]; and strong longitudinal ridges posterior to anterior tuberosities [Gentry's character 47(1)]. Furthermore, they differ in the following features: longer horncore in *Pantholops*; horncore with presence of deep longitudinal grooves in *Qurliqnoria*; horncore with clockwise torsion on the right side in *Qurliqnoria*; presence of postcornual fossa in *Qurliqnoria*; larger auditory bulla in *Qurliqnoria*; basioccipital variably triangular or rectangular in *Qurliqnoria*, more rectangular in *Pantholops*; and less laterally facing occipital surface in *Qurliqnoria* and less laterally facing mastoid exposure in *Pantholops*.

Gentry (2000) evaluated morphological evidence that united *Pachytragus* with caprins (formerly Caprinae). Here, we use the relevant points he brought up to evaluate the affinity of *Qurliqnoria* with caprins. The anterior keel on the horncores of *Qurliqnoria*, where observed, tend to originate proximally at an anteromedial position and move outward distally as the horncore rotates along its length. This anteromedial origin of the keel is similar to that in modern goats and *Pachytragus*. The elevation of the frontal bones between the horncores is observed in *Pachytragus* and modern Caprini, but the feature is weak in *Qurliqnoria*. The inclination of the cranial roof when the occipital plane is placed vertically is high in *Qurliqnoria*, like caprins and *Pachytragus*. The braincase of *Qurliqnoria* is rectangular in overall profile, without anterior widening, as seen in *Pachytragus* and caprins. The ratio of the distance between the supraorbital foramina to the distance between the lateral sides of the horn pedicel is 35%. The posterior wall of the bulla descends to come into contact with the paroccipital process, which is a basal condition seen in caprins as interpreted by Gentry (1992). Two cranial apomorphies of Caprini plus *Pachytragus* pointed out by Gentry (2000) are the elevation of the frontals between the horncores and the anterior widening of the braincase; both of these are more evident in living *Pantholops* than in *Qurliqnoria*. Given the basal cranial features of *Qurliqnoria* in comparison to both *Protoryx* and *Pachytragus*, which
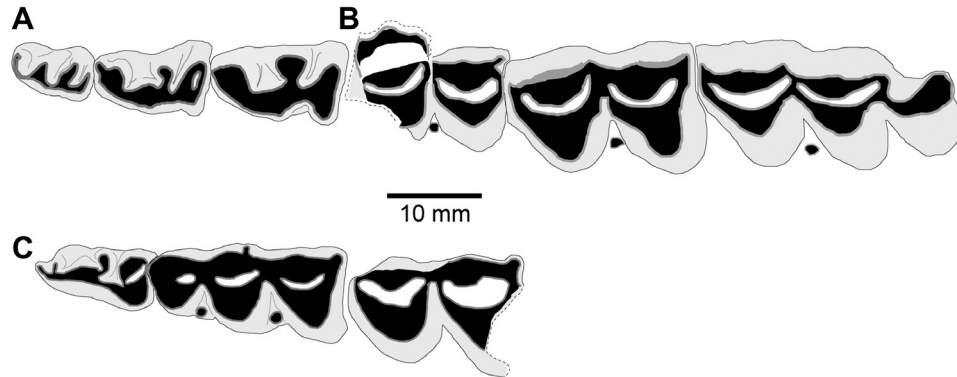
Figure 12. Composite lower toothrow of cf. *Qurliqnoria cheni* from Qaidam Basin. A, IVPP V16961. B, IVPP V16954. C, IVPP V16956.

Table 4. Lower tooth measurements of some Middle and Late Miocene bovids

Tooth	*Tethytragus koehlerae*	*Tethytragus langai*	*Gentrytragus gentryi*	cf. *Qurliqnoria cheni* (IVPP)			*Pachytragus crassicornis*	*Protoryx carolinae*
	Çandir	Val-Barranca	Ngorora	V16954	V16956	V16961	Akkaşdaği	M10366
Lp2	5.9–8.6 (38)	7.8–7.9 (3)	7.0	–	–	8.8	9.6–10.5 (6)	14.95
Wp2	3.0–4.9 (36)	4.0–5.2 (3)	4.0	–	–	6.7	5.5–6.1 (6)	8.35
Lp3	8.0–10.8 (71)	9.8–10.6 (5)	9.6–11.0 (3)	–	12.2	12.7	11.0–12.2 (7)	18.15
Wp3	3.9–6.2 (71)	6.0–6.9 (5)	5.5–6.5 (3)	–	6.3	7.8	7.0–7.6 (7)	11.7
Lp4	6.2–11.9 (90)	11.4–12.7 (7)	11.6–13.2 (3)	–	d20.1	13.9	13.3–14.5 (6)	20.4
Wp4	5.4–6.8 (93)	7.1–8.3 (7)	7.9–8.6 (3)	–	d9.3	8.7	7.6–8.2 (7)	13.35
Lm1	9.3–11.9 (90)	12.2–13.7 (4)	13.8–16.4 (2)	16.1	17.4	15.1	15.5–17.5 (9)	20.8
Wm1	6.6–9.0 (93)	8.4–8.8 (4)	10.4–11.3 (2)	9.9	12.5	11.3	9.9–11.7 (9)	16.2
Lm2	11.1–13.9 (97)	13.3–15.4 (6)	18.0–22.3 (4)	19.7	–	–	18.3–20.3 (6)	23.7
Wm2	7.1–9.6 (95)	8.5–9.7 (7)	11.7–13.4 (4)	13.3	–	–	11.4–12.8 (7)	16
Lm3	16.0–19.5 (72)	18.2–20.8 (10)	26.7–29.3 (2)	26.6	–	–	26.0–27.4 (4)	32.3
Wm3	7.1–9.2 (76)	8.6–9.8 (10)	11.4–11.5 (2)	12.8	–	–	10.1–11.9 (4)	17.2

Data for *Tethytragus* and *Gentrytragus* are from Azanza & Morales (1994), *Pachytragus* from Kostopoulos (2005) and *Protoryx* from Pilgrim & Hopwood (1928). All measurements are in millimetres. Abbreviation: d, deciduous tooth.

are early fossil members of the Caprini according to Gentry (2000), *Qurliqnoria* would fall outside the clade phylogenetically. This basal position for *Qurliqnoria* is consistent with Gentry's (1968) assessment of the genus as an extinct relative of *Pantholops* and with recent morphological, behavioural and molecular analyses that place *Pantholops* as a genus sister to caprins (Vrba & Schaller, 2000; Hernández Fernández & Vrba, 2005; but see Feng *et al.*, 2008).

Dental material

Only one of the top four most parsimonious trees from analyses of the dental morphological characters coded from cf. *Q. cheni* specimens indicates a relationship to *Pantholops* plus caprins (Fig. 14). The other top-performing trees place cf. *Qurliqnoria* as stem to all other Antilopinae or to Hippotragini–Alcepaphini–Caprini–Reduncini. All other constraint scenarios received lower support (higher parsimony score).

These results indicate that dentitions referred to *Qurliqnoria* are not as unequivocally grouped with *Pantholops* as in top-performing analyses using cranial and horncore characters. Additional sensitivity analyses coding both cranial and dental characters for *Q. cheni* and *Qurliqnoria* cf. *Q. cheni* as a single taxon returned results that are similar to those obtained in the cranial-only data partition.

On a qualitative level, the dental morphology of cf. *Qurliqnoria* jaw specimens suggests an overall evolutionary stage more derived than *Tethytragus*, but
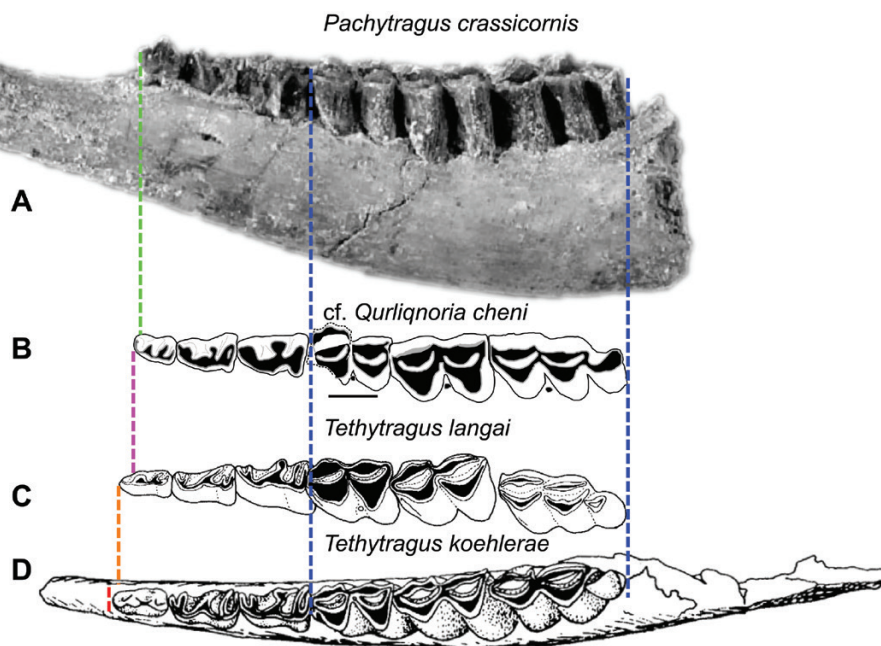
Figure 13. Comparison of premolar–molar toothrow ratios in several fossil bovids. A, *Pachytragus crassicornis* (modified from Kostopoulos, 2005). B, cf. *Qurliqnoria cheni* (composite of IVPP V16961 and IVPP V16954). C, *Tethytragus langai* (modified from Azanza & Morales, 1994). D, *Tethytragus koehlerae* (modified from Geraads, 2003). Toothrow lengths are scaled to molar 1–3 lengths. Scale bar: 10 mm in B, for cf. *Q. cheni* only. Blue dashed lines delineate the molar region of the toothrow. Other colours indicate relative lengthening of the premolar toothrow from A to D.

possessing a suite of both derived and basal characters shared with *Protoryx* and *Pachytragus* (Figs 12, 13), which share morphological similarities with other Chinese bovids, such as *Dorcadoryx*, *Huabeitragus* and *Macrotragus*.

DISCUSSION

A substantial fossil sample of the Late Miocene *Q. cheni* from the Qaidam Basin of the Tibetan Plateau provides new cladistic and quantitative evidence for a deep-time connection between the fossil bovid and the living *Pantholops*. The previously proposed *Pantholops*–Caprini sister-group relationship and 10–12 Mya as the lower bound for the appearance of that clade (Bibi *et al.*, 2013) are supported by the new data. The presence of Middle Miocene bovids, such as *Tethytragus* and *Gentrytragus*, in Europe and their possible position at the base of the divergence of Caprini, Hippotragini and Alcelaphini (Bibi *et al.*, 2009) suggest that the *Qurliqnoria*–*Pantholops* lineage might have diverged from other fossil bovids in Europe and dispersed to Central Asia.

The possibility of certain parts of the Tibetan Plateau reaching present-day elevations by the Middle Miocene suggests that *Qurliqnoria* predecessors already possessed the physiological characteristics required for dispersing

onto, and surviving on, the Tibetan Plateau, which was already close to present-day elevations and environmental conditions (Deng & Ding, 2015). Such an 'into Tibet' dispersal event precedes two other recently documented instances in Pliocene siphneid and cricetid rodents (Li & Wang, 2015; Li *et al.*, 2017). These events suggest the intermittent presence of barriers to inward dispersal to the Plateau and yet undetermined geographical factors that shaped the modern-day Plateau faunas. Recent discoveries of additional fossils assigned to *Qurliqnoria* in Turkey, and possibly Greece, suggest a more complex dispersal history of relatives (or descendants) of *Q. cheni* to regions beyond the Plateau (Kostopoulos *et al.*, 2020). A comprehensive review of all available Eurasian *Qurliqnoria* material is needed to pinpoint the timing and potential adaptations that allowed *Qurliqnoria* to thrive in a wide range of environments, from high-elevation tundra to low-lying coastal regions.

The palaeogeographical association of *Q. cheni* to the Tibetan Plateau area and its link to *Pantholops* indicate *in situ* evolution on the Plateau during the past 12–10 Myr. The discovery of dental materials tentatively assigned to *Qurliqnoria* supports the placement of *Qurliqnoria* basal to caprins and near *Pantholops*. The long evolutionary history on the Tibetan Plateau of chiru, much longer than any other living mammals found there, permitted accumulation of adaptations to an increasingly inhospitable plateau that
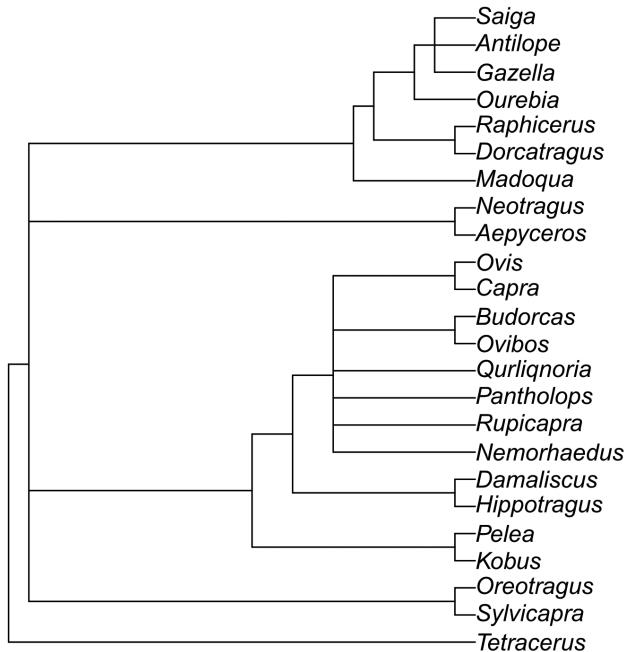
Figure 14. Most parsimonious phylogeny using dental characters coded for cf. *Qurliqnoria*. Mitochodrial DNA backbone constraint from Bibi (2013) with only monophyly of tribes enforced (topology within tribes unconstrained) and with *Qurliqnoria* within a Caprini + *Pantholops* clade. For tree scores and additional sensitivity analyses, see main text (scenario C) and Table 1.

became higher, colder and drier, with morphological and behavioural traits, such as air sacs in the nasal passage and seasonal female migrations, possibly inherited from their distant ancestors (Schaller, 1998). The deep endemism of the Tibetan antelope lineage suggests an association and even reliance of the *Qurliqnoria–Pantholops* lineage on harsh Plateau environments that might not be replaceable in peripheral regions. These observations are consistent with the physical forcing hypothesis for evolutionary novelties in species adaptation to harsh environments (Fortelius *et al.*, 2014), and the prediction that endemism occurring in tectonically active regions, such as the Tibetan Plateau, exemplifies *in situ* evolution rather than range reduction (Badgley, 2010). The new fossil data therefore provide an important palaeobiological context to inform the management of this near-threatened species in the face of accelerating climatic changes.

ACKNOWLEDGEMENTS

REFERENCES

Azanza B, **Morales J. 1994.** *Tethytragus* nov. gen. et *Gentrytragus* nov. gen. Deux nouveaux bovidés (Artiodactyla, Mammalia) du Miocène moyen. Relations phylogénétiques des Bovidés anté-vallésiens. *Proceedings of the Koninklijke Nederlandse Akademie van Wetenschappen* **97:** 249–282.

Badgley C. 2010. Tectonics, topography, and mammalian diversity. *Ecography* **33:** 220–231.

Barnosky AD, **Hadly EA**, **Gonzalez P**, **Head J**, **Polly PD**, **Lawing AM**, **Eronen JT**, **Ackerly DD**, **Alex K**, **Biber E**, **Blois J**, **Brashares J**, **Ceballos G**, **Davis E**, **Dietl GP**, **Dirzo R**, **Doremus H**, **Fortelius M**, **Greene HW**, **Hellmann J**, **Hickler T**, **Jackson ST**, **Kemp M**, **Koch PL**, **Kremen C**, **Lindsey EL**, **Looy C**, **Marshall CR**, **Mendenhall C**, **Mulch A**, **Mychajliw AM**, **Nowak C**, **Ramakrishnan U**, **Schnitzler J**, **Das Shrestha K**, **Solari K**, **Stegner L**, **Stegner MA**, **Stenseth NC**, **Wake MH**, **Zhang Z. 2017.** Merging paleobiology with conservation biology to guide the future of terrestrial ecosystems. *Science* **355:** eaah4787.

Bibi F. 2013. A multi-calibrated mitochondrial phylogeny of extant Bovidae (Artiodactyla, Ruminantia) and the importance of the fossil record to systematics. *BMC Evolutionary Biology* **13:** 166.

Bibi F, **Bukhsianidze M**, **Gentry A**, **Geraads D**, **Kostopoulos D**, **Vrba E. 2009.** The fossil record and evolution of Bovidae: state of the field. *Palaeontologia Electronica* **12:** 10A.

Bibi F, **Güleç E. 2008.** Bovidae (Mammalia: Artiodactyla) from the late Miocene of Sivas, Turkey. *Journal of Vertebrate Paleontology* **28:** 501–519.

Bohlin B. 1935a. *Tsaidamotherium hedini*, n. g., n. sp. *Geografiska Annaler* **17:** 66–74.

Bohlin B. 1935b. Carnivores der *Hipparion*-fauna Nord Chinas. *Palaeontologia Sinica Series C* **9:** 1–166.

Bohlin B. 1937. Eine tertiäre Säugetier-Fauna aus Tsaidam. *Sino-Swedish Expedition Publication (Palaeontologia Sinica Series C)* **14:** 3–111.

Bohlin B. 1945. Palaeontological and geological researches in Mongolia and Kansu 1929–1933. *Sino-Swedish Expedition Publication* **26:** 257–325.

Chen GF. 2005. *Dorcadoryx* Teilhard et Trassaert, 1938 (Bovidae, Artiodactyla) from the Bahe Formation of Lantian, Shaanxi Province, China. *Vertebrata PalAsiatica* **43:** 272–282.

Chen GF, **Zhang Z. 2007.** Restudy of Chinese fossil bovids referred to *Protoryx* (Bovidae, Artiodactyla). *Vertebrata PalAsiatica* **45:** 98–109.

Deng T, **Ding L. 2015.** Paleoaltimetry reconstructions of the Tibetan Plateau: progress and contradictions. *National Science Review* **2:** 417–437.

Deng T, **Wang X**, **Fortelius M**, **Li Q**, **Wang Y**, **Tseng ZJ**, **Takeuchi GT**, **Saylor JE**, **Säilä LK**, **Xie G. 2011.** Out of Tibet: Pliocene woolly rhino suggests high-plateau origin of Ice Age megaherbivores. *Science* **333:** 1285–1288.

Dietl GP. 2016. Brave new world of conservation paleobiology. *Frontiers in Ecology and Evolution* **4:** 21.

Fang X-M, **Zhang W-L**, **Meng Q-Q**, **Gao J-P**, **Wang X-M**, **King J**, **Song C-H**, **Dai S**, **Miao Y-F. 2007.** High-resolution magnetostratigraphy of the Neogene Huaitoutala section in the eastern Qaidam Basin on the NE Tibetan Plateau, Qinghai Province, China and its implication on tectonic uplift of the NE Tibetan Plateau. *Earth and Planetary Science Letters* **258:** 293–306.

Feng Z, **Fan B**, **Li K**, **Zhang QD**, **Yang QS**, **Liu B. 2008.** Molecular characteristics of Tibetan antelope (*Pantholops hodgsonii*) mitochondrial DNA control region and phylogenetic inferences with related species. *Small Ruminant Research* **75:** 236–242.

Field DJ, **Hsiang AY. 2018.** A North American stem turaco, and the complex biogeographic history of modern birds. *BMC Evolutionary Biology* **18:** 102.

Fortelius M, **Eronen JT**, **Kaya F**, **Tang H**, **Raia P**, **Puolamäki K. 2014.** Evolution of Neogene mammals in Eurasia: environmental forcing and biotic interactions. *Annual Review of Earth and Planetary Sciences* **42:** 579–604.

Ge R-L, **Cai Q**, **Shen YY**, **San A**, **Ma L**, **Zhang Y**, **Yi X**, **Chen Y**, **Yang L**, **Huang Y**, **He R**, **Hui Y**, **Hao M**, **Li Y**, **Wang B**, **Ou X**, **Xu J**, **Zhang Y**, **Wu K**, **Geng C**, **Zhou W**, **Zhou T**, **Irwin DM**, **Yang Y**, **Ying L**, **Bao H**, **Kim J**, **Larkin DM**, **Ma J**, **Lewin HA**, **Xing J**, **Platt RN**, **Ray DA**, **Auvil L**, **Capitanu B**, **Zhang X**, **Zhang G**, **Murphy RW**, **Wang J**, **Zhang YP**, **Wang J. 2013.** Draft genome sequence of the Tibetan antelope. *Nature Communications* **4:** 1858.

Gentry AW. 1968. The extinct bovid genus *Qurliqnoria* Bohlin. *Journal of Mammalogy* **49:** 769–769.

Gentry AW. 1971. The earliest goats and other antelopes from the Samos *Hipparion* fauna. *Bulletin of the British Museum (Natural History) (Geology)* **20:** 229–296.

Gentry AW. 1990. Ruminant artiodactyls of Paşalar, Turkey. *Journal of Human Evolution* **19:** 529–550.

Gentry AW. 1992. The subfamilies and tribes of the family Bovidae. *Mammal Review* **22:** 1–32.

Gentry AW. 2000. Caprinae and Hippotragini (Bovidae, Mammalia) in the Upper Miocene. In: Vrba ES, Schaller GB, eds. *Antelopes, deer, and relatives: fossil record, behavioral ecology, systematics, and conservation*. New Haven: Yale University Press, 65–83.

Gentry AW. 2003. Ruminantia (Artiodactyla). In: Fortelius M, Kappelman J, Sen S, Bernor RL, eds. *Geology and paleontology of the Miocene Sinap Formation, Turkey*. New York: Columbia University Press, 332–379.

Geraads D. 2003. Ruminants, other than Giraffidae from the middle Miocene hominoid locality of Çandir (Turkey). *Courier Forschungsinstitut Senckenberg* **240:** 181–199.

Goloboff P, **Catalano S. 2016.** TNT, version 1.5, with a full implementation of phylogenetic morphometrics. *Cladistics* **32:** 221–238.

Hernández Fernández M, **Vrba ES. 2005.** A complete estimate of the phylogenetic relationships in Ruminantia: a dated species-level supertree of the extant ruminants. *Biology Reviews* **80:** 269–302.

IUCN SSC Antelope Specialist Group. **2016.** Pantholops hodgsonii. *The IUCN Red List of Threatened Species 2016: e.T15967A50192544*. Available at: https://dx.doi.org/10.2305/IUCN.UK.2016-2.RLTS.T15967A50192544.en

Kassambara A, **Mundt F. 2020.** *Factoextra: extract and visualize the results of multivariate data analyses. R package version 1.0.7*. Available at: https://CRAN.R-project.org/package=factoextra

Köhler VM. 1987. Boviden des türkischen Miozäns (Känozoikum und Braunkohlen der Türkei. 28). *Paleontologia i Evolució* **21:** 133–246.

Kostopoulos DS. 2005. The Bovidae (Mammalia, Artiodactyla) from the late Miocene of Akkaşdaği, Turkey. *Geodiversitas* **27:** 747–791.

Kostopoulos DS, **Erol AS**, **Mayda S**, **Yavuz AY**, **Tarhan E. 2020.** *Qurliqnoria* (Bovidae, Mammalia) from the Upper Miocene of Çorakyerler (Central Anatolia, Turkey) and its biogeographic implications. *Palaeoworld* **29:** 629–635.

Leclerc C, **Bellard C**, **Luque GM**, **Courchamp F. 2015.** Overcoming extinction: understanding processes of recovery of the Tibetan antelope. *Ecosphere* **6:** 171.

Lee MSY. 2013. Turtle origins: insights from phylogenetic retrofitting and molecular scaffolds. *Journal of Evolutionary Biology* **26:** 2729–2738.

Leslie DM, **Schaller GB. 2008.** *Pantholops hodgsonii* (Artiodactyla: Bovidae). *Mammalian Species* **817:** 1–13.

Li Q, **Stidham T**, **Ni X**, **Li L. 2017.** Two new Pliocene hamsters (Cricetidae, Rodentia) from southwestern Tibet (China), and their implications for rodent dispersal 'into Tibet'. *Journal of Vertebrate Paleontology* **37:** 6.

Li Q, **Wang X. 2015.** Into Tibet: an early Pliocene dispersal of fossil zokor (Rodentia: Spalacidae) from Mongolian Plateau to the hinterland of Tibetan Plateau. *PLoS One* **10:** e0144993.

Li Q, **Xie G-P**, **Takeuchi GT**, **Deng T**, **Tseng ZJ**, **Grohé C**, **Wang X. 2014.** Vertebrate fossils on the roof of the world: biostratigraphy and geochronology of high-elevation Kunlun Pass Basin, northern Tibetan Plateau, and basin history as related to the Kunlun strike-slip fault. *Palaeogeography, Palaeoclimatology, Palaeoecology* **411:** 46–55.

Lydekker R. 1901. On the skull of a chiru-like Antelope from the ossiferous deposits of Hundes (Tibet). *Quarterly Journal of the Geological Society* **57:** 289–292.

Maddison WP, **Maddison DR. 2009.** *Mesquite: a modular system for evolutionary analysis. Version 2.71*. Available at: http://mesquiteproject.org

Mathews S, **Clements MD**, **Beilstein MA. 2010.** A duplicate gene rooting of seed plants and the phylogenetic position of flowering plants. *Philosophical Transactions of the Royal Society B: Biological Sciences* **365:** 383–395.

Ozansoy F. 1957. Faunes de mammifères du Tertiaire de Turquie et leurs révisions stratigraphiques. *Bulletin of the Mineral Research and Exploration Institute of Turkey* **49:** 29–48.

Ozansoy F. 1958. *Étude des gisements continentaux et des mammifères du Cénozoique de Turquie*. Paris: Faculté de Sciences, Université de Paris.

Pei J, **Wang L**, **Xu W**, **Kurz DJ**, **Geng J**, **Fang H**, **Guo X**, **Niu Z**, **2019.** Recovered Tibetan antelope at risk again. *Science* **366**(6462): 194.

Pilgrim GE, **Hopwood AT. 1928.** *Catalogue of the Pontian Bovidae of Europe*. London: British Museum (Natural History).

Qiu ZX, **Yie J**, **Jiang YJ. 1987.** Some mammalian fossils of Bahe stage from Wuzhong, Ningxia. *Vertebrata PalAsiatica* **25:** 46–56.

Rawling CG. 1905. *The Great Plateau. Being an account of exploration in Central Tibet, 1903, and of the Gartok Expedition, 1904–1905*. London: Edward Arnold.

Schaller GB. 1998. *Wildlife of the Tibetan steppe*. Chicago: University of Chicago Press.

Sen S. 2003. History of paleontologic research in Neogene deposits of the Sinap Formation, Ankara, Turkey. In: Fortelius M, Kappelman J, Sen S, Bernor RL, eds. *Geology and paleontology of the Miocene Sinap Formation, Turkey*. New York: Columbia University Press, 1–22.

Shen X, **Tian Q**, **Ding G**, **Wei K**, **Chen Z. 2001.** The Late Cenozoic stratigraphic sequence and its implication to tectonic evolution, Hejiakouzi Area, Ningxia Hui Autonomous Region. *Earthquake Research in China* **17:** 156–166.

Signore AV, **Storz JF. 2020.** Biochemical pedomorphosis and genetic assimilation in the hypoxia adaptation of Tibetan antelope. *Science Advances* **6:** eabb5447.

Solounias N, **Moelleken SMC. 1992.** Dietary adaptations of two goat ancestors and evolutionary consideration. *Geobios* **25:** 797–809.

Teilhard de Chardin P, **Trassaert M. 1938.** Cavicornia of south-eastern Shansi. *Palaeontologia Sinica Series C* **6:** 1–99.

Tseng ZJ, **Wang X**, **Slater GJ**, **Takeuchi GT**, **Li Q**, **Liu J**, **Xie G. 2014.** Himalayan fossils of the oldest known pantherine establish ancient origin of big cats. *Proceedings of the Royal Society B: Biological Sciences* **281**(1774): 20132686.

Vrba ES, **Schaller GB. 2000.** Phylogeny of Bovidae based on behavior, glands, skulls, and postcrania. In: Vrba ES, Schaller GB, eds. *Antelopes, deer and relatives: fossil record, behavioral ecology, systematics, and conservation*. New Haven: Yale University Press, 203–222.

Wang X, **Jukar AM**, **Tseng ZJ**, **Li Q. 2020.** Dragon bones from the heavens: European explorations and early palaeontology in Zanda Basin of Tibet, retracing type locality of *Qurliqnoria hundesiensis* and *Hipparion* (*Plesiohipparion*) *zandaense*. *Historical Biology* **33:** 2216–2227.

Wang X, **Li Q**, **Qiu Z-D**, **Xie G-P**, **Wang B-Y**, **Qiu Z-X**, **Tseng ZJ**, **Takeuchi GT. 2013.** Chapter 10. Neogene mammalian biostratigraphy and geochronology of the Tibetan Plateau. In: Wang X, Flynn LJ, Fortelius M, eds. *Fossil mammals of Asia: Neogene biostratigraphy and chronology*. New York: Columbia University Press, 274–292.

Wang X, **Qiu Z**, **Li Q**, **Wang B**, **Qiu Z**, **Downs WR**, **Xie G**, **Xie J**, **Deng T**, **Takeuchi GT**, **Tseng ZJ**, **Chang M**, **Liu J**, **Wang Y**, **Biasatti D**, **Sun Z**, **Fang X**, **Meng Q. 2007.** Vertebrate paleontology, biostratigraphy, geochronology, and paleoenvironment of Qaidam Basin in northern Tibetan Plateau. *Palaeogeography, Palaeoclimatology, Palaeoecology* **254:** 363–385.

Wang X, **Xie G**, **Qiu Z**, **Li Q**, **Tseng ZJ**, **Takeuchi GT**, **Wang B**, **Fortelius M**, **Fortelius A**, **Walhqvist H. 2011.** Early explorations of Qaidam Basin (Tibetan Plateau) by Birger Bohlin—reconciling classic vertebrate fossil localities with modern biostratigraphy. *Vertebrata PalAsiatica* **46:** 285–310.

Yin A, **Dang Y**, **Wang L-C**, **Jiang W-M**, **Zhou S-P**, **Chen X**, **Gehrels GE**, **McRivette MW. 2008a**. Cenozoic tectonic evolution of Qaidam basin and its surrounding regions (Part 1): the southern Qilian Shan-Nan Shan thrust belt and northern Qaidam basin. *Geological Society of America Bulletin* **120:** 813–846.

Yin A, **Dang Y**, **Zhang M**, **Chen X**, **McRivette MW. 2008b.** Cenozoic tectonic evolution of the Qaidam basin and its surrounding regions (Part 3): structural geology, sedimentation, and regional tectonic reconstruction. *Geological Society of America Bulletin* **120:** 847–876.

Yin A, **Dang Y**, **Zhang M**, **McRivette MW**, **Burgess WP**, **Chen X. 2007.** Cenozoic tectonic evolution of Qaidam Basin and its surrounding regions (part 2): wedge tectonics in southern Qaidam basin and the eastern Kunlun Range. *Geological Society of American Special Paper* **433:** 369–390.